LBL-7631

A STUDY OF PHONON-INDUCED ENERGY TRANSFER PROCESSES IN CRYSTALS USING HEAT PULSES

Alan Richard Burns
(Ph. D. thesis)

March 1978

Prepared for the U. S. Department of Energy
under Contract W-7405-ENG-48

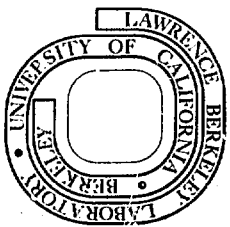

LBL-7631

TABLE OF CONTENTS

A STUDY OF PHONON-INDUCED ENERGY TRANSFER PROCESSES IN CRYSTALS USING HEAT PULSES

Alan Richard Burns

Materials and Molecular Research Division
and Department of Chemistry
Lawrence Berkeley Laboratory
University of California
Berkeley, California 94720

March 1978

Abstract

The artificial generation of acoustic lattice vibrations by a heat pulse technique is developed in order to probe phonon interactions in molecular crystals. Specifically, the phonon-assisted delocalization of "trapped" excited triplet state energy in the aromatic crystal 1,2,4,5-tetrachlorobenzene (TCB) is studied in a quantitative manner by monitoring the time-resolved decrease in trap phosphorescence intensity due to the propagation of a well-defined heat pulse.

The excitation distribution in a single trap system, such as the X-trap in neat h_2-TCB, is discussed in terms of the energy partition function relating

the temperature dependence of the trap phosphorescence intensity to the trap depth, exciton bandwidth, and the number of exciton band states. In a multiple trap system, such as the hd and h_2 isotopic traps in d_2-TCB, the excitation distribution is distinctly non-Boltzmann; yet it may be discussed in terms of a preferential energy transfer between the two trap states via the exciton band. For both trap systems, a previously developed kinetic model is presented which relates the efficiency of trap-band energy exchange to the density of band states and the trap-phonon coupling matrix elements.

The applicability of the heat pulse technique in molecular crystals is studied in terms of important phonon transmission parameters. The theory of phonon scattering in dielectric solids is briefly reviewed and extended to the case of molecular crystals in order to determine the feasibility of observing a size-limited phonon mean free path at low temperatures. In addition, the acoustic mismatch model for the thermal boundary conductance between dissimilar materials is presented and applied to the problem of the interface conductance between the molecular crystal and a thin-film nichrome heater.

A bolometric technique for determining the thermal response time of the heater/crystal system is presented. From the germanium bolometer data, and the heat capacity data obtained by an independent calorimetric experiment, the crystal lattice conductance and the heater/crystal conductance are calculated. The results indicate that the phonon mean free path in the crystal is in fact size-limited, and that the heater/crystal boundary conductance is reasonably close to previously reported values for similar systems. The response time of the trap phoshorescence modulation is shown to be directly related to the thermal response time of the crystal; thus the rate of delocalization of trapped excitations is limited by the rate at which phonons enter the crystal.

The theory of heat pulse phonon spectroscopy is presented and discussed in terms of black body phonon radiation. The broad-band spectrum of phonons emitted by the heater film can be studied by frequency-selective phonon absorption processes. Of special interest is the resonant absorption of phonons which leads to the delocalization of trapped excitations. The heat pulse power dependence of the trap phosphorescence modulation depth for three distinct traps is shown to be a function of the trap depth and the effective temperature of the black body radiator. The effective temperature , in turn, is found to be intimately related to the input power at the heater film and the heater/crystal boundary conductivity. A phonon absorption coefficient is then defined which relates the relative phosphorescence modulation depth to the resonant phonon flux. When the results from many single trap and multiple trap systems are compared, the absorption coefficient is found to be directly proportional to the density of states in the host band and the trap-phonon coupling efficiency.

Chapter I

Introduction

The absorbtion of light by molecules in a well-ordered crystal results in the creation of excited states that are a function of the collective nature of the crystal as a whole. If the crystal is free of all imperfections, then the excited states can be characterized solely by a band of energies centered around the level associated with the isolated molecule. The subsequent migration of the excited state energy from one region of the crystal to another can then be discussed in terms of the exciton theory formulated by Frenkel[1] and Davydov.[2] In any real crystal, however, there are always finite quantities of imperfections incorporated in the lattice. In many cases, the imperfections give rise to new excited states which are effectively removed from the band.[3] When these localized states are lower in energy than the exciton band, they can act as "traps." Thus a complete picture of energy migration in molecular solids must include a description of the process by which energy can be transferred from the molecule associated with the trap state to the host molecules comprising the band. Virtually every solid state phenomenon is coupled to the lattice; and excited state energy transfer is no exception. Indeed, the mechanism by which energy is transferred from traps to the band includes the intervention of a lattice phonon.

All the work presented in this thesis deals exclusively with the lowest energy triplet states of aromatic molecular crystals. There are various advantages and disadvantages of working with these systems, which will be brought up throughout the text, but the primary motivation in studying these systems is that many important features concerning the general problem of energy migration can be investigated by time-resolved methods utilizing optical detection. The relatively long lifetime (msec regime) of the excited triplet states allows one to conduct

a myriad of different experiments, each of which enjoys the sensitivity of photon detection, and which together help formulate a reasonable model for energy transfer processes.

In a molecular crystal such as 1,2,4,5-tetrachlorobenzene (TCB), there are three basic kinds of traps. The first are associated with chemical impurities, where the trap state is assigned either to the excited state of the impurity molecule itself, or with the perturbed host molecules in the vicinity of the impurity. In the former case, the energy difference between the excited state of the impurity and that of the host, the so-called trap "depth," may exceed several thousand wavenumbers. An example of the latter case is found in the chemically-induced Y-trap, which has a trap depth of approximately 50 cm^{-1}. A second kind of trap is also a structural perturbation, but it involves the more subtle character of a TCB molecule which is misaligned with respect to the translational symmetry of the lattice. This intrinsic mechanical imperfection gives rise to the X-trap, which has a depth below the exciton band of 17 cm^{-1}. The third class of traps are isotopic. These were originally pointed out by Nieman and Robinson[4]. In particular, if the host material is artificially deuterated, then small traces of residual protonated molecules will be distributed uniformly throughout the crystal. Although they will not affect the structure of the lattice, the isotopic impurities will have lower excited state energies by virtue of their differing zero point energies. Thus the hd-TCB and the h_2-TCB molecules in d_2-TCB are traps that have depths of 11 cm^{-1} and 22 cm^{-1}, respectively.

The primary concern of this thesis is to show: (1) that the promotion of the excited state energy from a trap to the band is a process that involves a lattice phonon which is resonant with the trap depth; (2) that the efficiency of the promotion process is directly proportional to the number of available

states in the band; and (3) that the efficiency is also sensitive to the nature of the trap. It has already been established[5] that the temperature dependence of the trap phoshorescence intensity can be used to analyze the partitioning of energy between the trap and the band states. A discussion of this analysis and its immediate appliction to the present work will be given in Chapter II. However, an experimental method had to be developed which directly probed the interactions of specific phonons with the trap states.

Ideally, the most direct way of controlling the number of phonons having a specific energy is to artificially generate them. In practice, this can be exceedingly difficult, but there are two general methods that have proven to be successful in studying a wide variety of phonon interactions in both metals and dielectrics, namely ultrasonic techniques and heat pulses. Ultrasonic generation of monochromatic acoustic phonons involves a microwave transduction that is usually limited to frequencies below 100 GHz (3 cm^{-1}), hence the promotion of trapped states which requires energies of 10 cm^{-1} or more is out of the ultrasonic generation range. However, the generation of high frequency phonons with energies exceeding 30 cm^{-1} or more can easily be obtained by the heat pulse technique. This is because the central frequency in the heat pulse spectrum is proportional to kT_H/h , where T_H is the heater temperature. The heat pulse technique has the disadvantage of using a very broad-band source of phonons, since the width about the central frequency is also proportional to kT_H/h. Despite this undesirable feature, if it can be shown that the phonon absorption and/or scattering processes are frequency-selective, then the coupling of a broad-band source, such as a simple heater, to a crystalline sample can yield the same information as that obtained with a monochromatic source.

In 1974, A.H. Francis and his co-workers[6,7] were the first investigators

to demonstrate that the phosphorescence intensity of trap emmision could be modulated by the application of a heat pulse. They were able to show that the depletion of the trap population and the simultaneous increase in the exciton population could be controlled by the amount of power dissipated in a small heater in thermal contact with a TCB crystal. At this time, however, it was believed that the heat pulse was simply a means to rapidly change the overall temperature of the lattice, such that when the pulse was over, the kinetics of the relaxation back to the original trap - band equilibrium distribution could be analyzed. Indeed, it was found that the shallower traps, due to their proximity to the exciton band, relaxed more rapidly to their steady-state population.

Since the experiments of Francis were the first to involve the application of heat pulses to a molecular crystal, many questions concerning the actual thermal response of the crystal lattice to the heat pulse modulation remained unanswered. Furthermore, the potential use of heat pulses to probe the phonon-mediated promotion event in a quantitative manner presented itself. In the process of confronting these problems, I realized that the heat pulse could be pictured more accurately as a phonon flux which propagated through the lattice and is partially absorbed by the traps. Once the nature of the phonon flux is established, then the quantitative, time-resolved, depletion of the trap population can be analyzed in terms of the various parameters which govern the exchange of energy between a trap molecule and the band.

In Chapter III, the general theory of heat pulse transmission in dielectric crystals is discussed with regard to the thermal conductivity of the lattice. The thermal contact between the crystal and a heater is discussed in terms of the thermal boundary conductance between dissimilar materials. In Chapter IV, the experimental results of a bolometric technique are used to discuss the thermal response of the heater/crystal system with respect to the theory presented in the previous chapter. Also in Chapter IV, the parameters governing the time

response of the trap phosphorescence modulation are discussed and compared with the bolometer results.

Since the phonon flux associated with a heat pulse can be characterized in terms of black body thermal radiation emitted by the heater, a general discussion of "phonon spectroscopy" is presented in Chapter V. Also in this chapter, the theory concerning the specific application of phonon spectroscopy to the problem of trap promotion is presented. In Chapter VI, the experimental phonon absorption coefficients for the promotion of X-traps and isotopic traps are presented. It will be shown that the absorption coefficient is not only a function of the density of available band states, but that it also reflects the nature of the trap.

Chapter II

Trap and Band Equilibria in Molecular Crystals

1. Single Trap Case

The phosphorescence spectrum of highly purified h_2-TCB at 1.5 K is shown in Fig.(1). At temperatures below 2.0 K, the emission spectrum consists primarily of the electronic origin and the vibronic progression from the 17 cm^{-1} X-trap and a small contribution from the exciton band. The exciton origin (0,0) is at 3748 Å and the X-trap origin is near 3751 Å. The first step in the vibronic progression is the b_{2g} origin at 3781 Å for the exciton and at 3784 Å for the X-trap.[8] At 4.2 K, the phosphorescence spectrum will consist solely of the exciton emission (inset). Thus over this temperature range, it is clear that the excited triplet state energy is partitioned between the X-trap and the exciton band.

TCB exhibits a lattice structure which is essentially a lamellar packing of the planar aromatic rings.[9] Since the interactions between neighboring molecules occur predominantly through the π electrons in the rings,[10] the transfer of excited triplet state energy in the band is primarily restricted to the direction along the axis of the lamellar stack. Because of this anisotropy, the lattice is often described as being "one-dimensional." The physics is greatly simplified, for the dispersion of the one-dimensional exciton band is reduced to

$$(1)\quad E(K) = E^0 + 2\beta \cos Ka \ ,$$

where β is the intermolecular interaction energy between nearest-neighbor molecules, a is the distance between translationally equivalent molecules, and E^0 is the excited state energy of the isolated molecule. The wavevector K varies

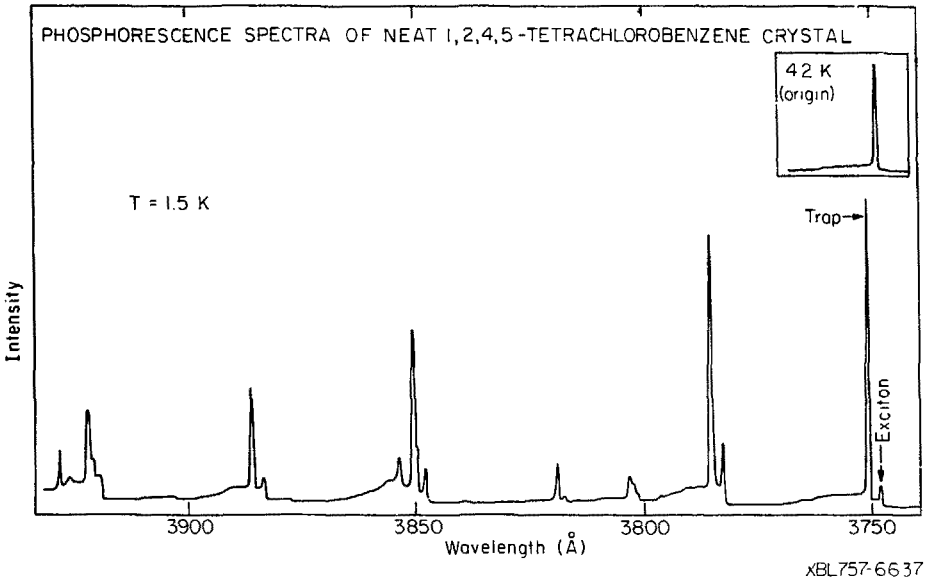

Fig. 1 Phosphorescence spectrum of neat h_2-TCB displaying X-trap emission and exciton emission.

from 0 to $\pm \pi/a$. If there is an average of 2n + 1 molecules in any given molecular chain between traps, there will be n doubly degenerate K states in the exciton band (the K=0 state is non-degenerate). The width of the exciton band is equal to 4β ; and since $\beta>0$, the K=0 level is located at the top of the band. The trap depth Δ is determined spectroscopically with respect to the K=0 level, thus the minimum energy difference between the trap state and the exciton band is equal to $\Delta - 4\beta$.

If one sets the zero of energy at the middle of the band, then the partition function for the excited state trap and band system at thermal equilibrium is given by: [5]

$$(2)\quad Z = \exp\left[-(2\beta - \Delta)/kT\right] + \sum_{K=-(n-1)/an}^{(n-1)/an} \exp\left[-(2\beta\cos Ka)/kT\right] \quad .$$

The first term in Eq.(2) represents the trap energy, and the summation is over all the band states. Since the number of band states usually exceeds 10^3 in a reasonably pure crystal, the summation can be approximated by an integral which has the form of the following zero-order modified Bessel function of the first kind:

$$(3)\quad I_0(\alpha) = (1/\pi) \int_0^{\pi} \exp(\alpha\cos\theta)d\theta \quad .$$

Then Eq.(2) can be rewritten as

$$(4)\quad Z = \exp\left[-(2\beta - \Delta)/kT\right] + nI_0(2\beta/kT) \quad .$$

Thus the probability of finding an excitation in the trap is given by

$$(5)\quad P_{trap} = \frac{\exp\left[-(2\beta - \Delta)/kT\right]}{Z} \quad .$$

The intensity of the trap emission, I, is equal to the product of the radiative rate constant K_r and the trap population N:

(6) $I = K_r N$.

Since K_r is temperature independent, and since the total number of excited states is constant under steady-state conditions, the intensity of the trap emission is directly proportional to the trapping probablity P_{trap}. Thus if the bandwidth and the spectroscopic trap depth are known, the temperature dependence of the trap phosphorescence intensity will yield the number of band states n.

An experimental value of $4\beta = 1.3\ cm^{-1}$ for TCB has been reported by Francis and Harris[11] in their study of the lineshape of the triplet $D + |E|$ band-to-band microwave transition. Dlott and Fayer[12] also reported that the TCB bandwidth of $1.3\ cm^{-1}$, along with a value for the spectroscopic trap depth $\Delta = 17.3\ cm^{-1}$, was used to fit their X-trap phosphorescence intensity measurements. In the present work, Δ was measured from the spectra of several different h_2-TCB samples and was found in each case to be roughly $17.3 \pm 0.3\ cm^{-1}$. The temperature dependences of the X-trap phosphorescence intensity for two of these samples are shown in Fig. (2). Unfortunately, the presence of bubbles in the He bath above the lambda point (2.17 K) reduces the light intensity of the emission by more than 30%; thus all the data that was used in the curve -fitting was taken at temperatures below the lambda point of liquid He. The curves which best-fit these data points were calculated from Eq.(5), where $4\beta = 1.3\ cm^{-1}$ and $\Delta = 17.3\ cm^{-1}$. Although the $\pm 0.30\ cm^{-1}$ error in the trap depth can translate into an error for n as large large as $\pm$ 10,000 states, it is evident that the number of band states can change appreciably from one crystal to the next. This situation is expected,however, since the X-trap is an intrinsic structural defect that can have a wide range

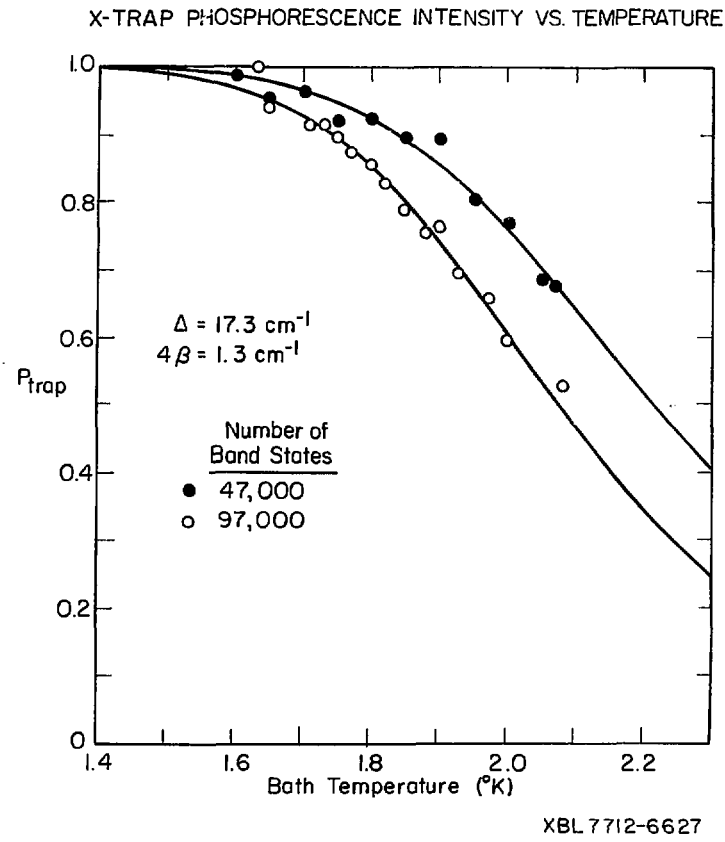

Fig. 2 Bath temperature dependence of the X-trap phosphorescence intensity (peak height) for two different neat h_2-TCB crystals. The number of exciton band states in each crystal is found by fitting the normalized data points to curves calculated from Eq. (5) when the trap depth Δ and the exciton bandwidth 4β are known.

of possible concentrations. Since the X-trap concentration is not affected by the presence of chemical impurities, the only way that it can be varied is through the extent by which the crystal is annealed.

2. Multiple Traps Case

In the preceeding section, it was shown that Boltzmann statistics can be used to fit the temperature dependence of the phosphorescence intensity of a single trap in the TCB lattice. Thermal equilibrium in this system is attained by the continuous exchange of energy between the trap and the band. If one looks at the process in detail[5], one recognizes that as soon as a trapped excitation is promoted to the band, there will be a net loss in the total trap population unless there is another excitation in the band that gets trapped. Thus equilibrium is established by promotion, migration in the band, and retrapping, in a time scale which is competitive with the radiative and non-radiative decay rates of the excited state.

If there are two traps in the lattice, each having a different depth below the exciton band, then the process of promotion, migration, and retrapping manifests itself in such a way as to produce a non-Boltzmann excitation distribution between the two traps. This phenomenon is evident in the phosphorescence intensity temperature dependences of the isotopic traps in d_2-TCB. One can see in Fig.(3) that the population of the "deep," 22 cm^{-1}, h_2-TCB trap increases when the bath temperature is raised. There is also a sharp decrease in the population of the "shallow," 11 cm^{-1}, hd-TCB trap. At temperatures below 2.0 K, the total emission intensity from both traps is fairly constant; thus there is a net transfer of excited state energy from the shallow trap to the deep trap as the bath temperature increases. The loss of population from the shallow trap

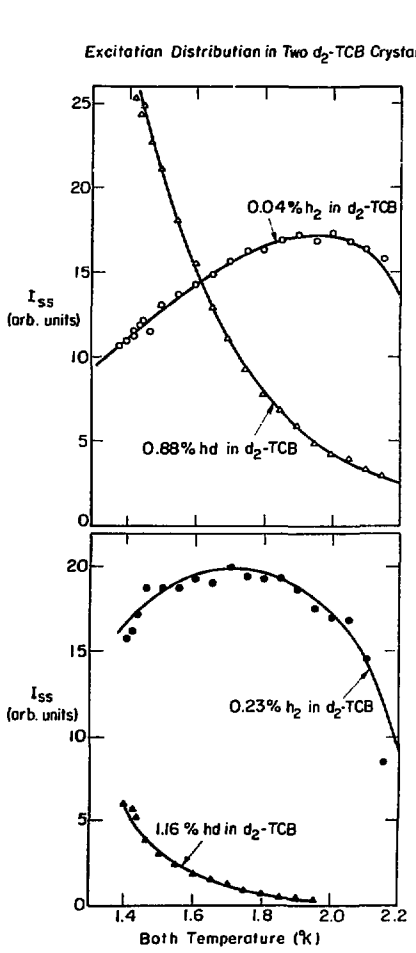

Fig. 3 Non-Boltzmann bath temp. dependence of the excitation distribution between the hd (11 cm^{-1}) and the h_2 (22 cm^{-1}) isotopic traps in two perdeuterated TCB crystals. White circles and triangles: 99.1% d_2-TCB. Black circles and triangles: 98.6% d_2-TCB.

is even more pronounced when the concentration of the deep trap is higher, as can be seen when one compares the data for the two d_2-TCB crystals shown in Fig. (3). At even greater h_2 concentrations, such as in the 0.78% and 5.4% h_2 crystals which will be discussed later on, practically all of the excitation energy resides in the deep trap. (All isotope concentrations are in terms of mole %).

The depletion of the shallow trap population and the build-up of the deep trap population are due to the fact that the shallow trap exchanges energy with the molecules in the band at a much faster rate than does the deep trap. If one relates the trap-band energy exchange rate with the trap depth, then it is clear that the shallower traps are able to "see" more phonons which have sufficient energy to cause thermal promotion than do deep traps. It remains to be seen, however , if the thermal promotion event requires phonons which are actually resonant with the trap depth.

Since Boltzmann statistics cannot be used to analyze the multiple traps system, one cannot estimate the number of band states from the phosphorescence temperature dependence. Thus one is restricted to samples where the concentration of the traps (isotopic or any other type), is known beforehand. When this is the case, one usually associates the number of band states with the ratio of the host concentration to the total guest concentration. In the 0.88% hd, 0.23% h_2 crystal, the ratio of host molecules to trap molecules is about 110; for the 1.16% hd, 0.23% h_2, crystal this ratio is approximately 72. The other two crystals that were used are 1.42%hd, 0.78% h_2, (42 band states), and 1.6% hd, 5.4% h_2 (14 band states). The vast difference in the number of band states between the single X-trap system and the isotopic systems will prove to be an interesting point in the discussion of the kinetics of trap-to-band energy transfer.

3. Kinetics of Trap-to-Band Energy Transfer

It was stressed in section 1 that the rate of thermal promotion of the localized trap state to a mobile exciton must be greater than the decay rate of the excitation ($27\ sec^{-1}$). In the model presented by Fayer and Harris[5], the promotion is viewed as a two-step process involving an intermediate state $|\tau_i\rangle$, which is isoenergetic with a state E_i in the band. A schematic of the process is shown in Fig. (4). In the first step, a phonon $P(\varepsilon)$ couples with the trap state $\langle\tau|$ to form the intermediate $|\tau_i\rangle$. The probability of forming the intermediate state is given by the matrix element $\langle\tau,P|\ H_{\tau P}\ |\tau_i\rangle$, weighted by the average number of phonons present which have an energy ε. If $\rho_p(\varepsilon)$ is the density of phonon states at energy ε, then the average number of phonons at ε is equal to the product of $\rho_p(\varepsilon)$ and the Planck distribution at temperature T. The second step in the promotion process involves the decay of the intermediate state into an exciton state $|E\rangle$ which has an energy E_i. The probability of this step is governed by the matrix element $\langle\tau_i|\ H_{iE}|E\rangle$, weighted by the density of available band states ρ_E at energy E_i.

The total probability per unit time for the delocalization of the trapped excitation takes the form of a Golden Rule rate constant obtained by summing over all the phonon energies ε resonant with the trap depth and by summing over all the states in the exciton band:

$$(7)\quad K_0 = \frac{2\pi}{\hbar}\int\rho_p(\varepsilon)d\varepsilon\left[\frac{1}{\exp(\varepsilon/kT)\ -\ 1}\right]\int\rho_E(E_i)dE_i$$
$$\times\ |\langle\tau,P|\ H_{\tau P}\ |\tau_i\rangle\langle\tau_i|\ H_{iE}\ |E_i\rangle|^2 \quad .$$

For a direct single phonon process, the first integral would be evaluated over the energy range $\Delta - 4\beta \rightarrow \Delta$. If the promotion rate constant is also depen-

SINGLE PHONON PROMOTION PROCESS

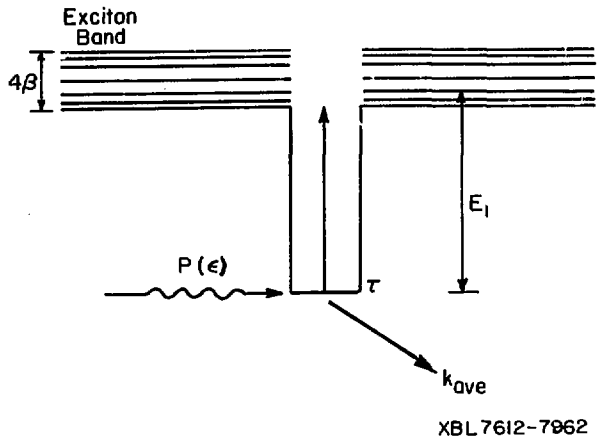

Fig. 4 Kinetic model for the single phonon-assisted promotion of a localized trap state ι to a state E_i isoenergetic with the exciton band. The energy ε of the phonon P is resonant with the trap depth. The width of the exciton band 4β is a function of the intermolecular interaction energy. The $K = 0$ state is at the top of the band, and the $K = \pm\pi/a$ states are at the bottom of the band. k_{ave} is the average radiative rate constant of the three triplet sublevels.

dent on multiphonon processes, such as the simultaneous absorbtion of low energy phonons or a Raman-type process involving high energy phonons, then Eq. (7) must be modified. At this point, however, it will be assumed that the promotion event involves only a single phonon. Further discussion about the possibility of actually observing multiphonon promotion processes will be given in Chapter VI.

In the absence of K-selective trap-exciton transitions, the matrix elements in Eq. (7) can be separated from the summation over the exciton band states E_i, such that the integral will give the total number of band states n. However, since the one-dimensional exciton density of states function $\rho_E(E_i)$ has maximum values at K=0 and K= $\pm$ π/a, one might anticipate that the promotion to the top and the bottom of the band would be dominant. Thus one would want to weight the phonons corresponding to these energies more heavily than those phonons having energies corresponding to the middle of the band. It will be shown in Chapter VI that this consideration is of little importance due to the small width of the exciton band relative to the trap depths under study. Thus the overall rate constant K_0 can be envisioned as being a quantity which is directly proportional to the number of phonons having energies in the range determined by the trap depth and and the exciton band width. K_0 will also be directly proportional to the number of band states, and the coupling matrix elements.

Lewellyn, Zewail, and Harris [13] used the technique of optically - detected spin coherence to measure a promotion rate constant of ~400 sec^{-1} for the 0.06% h_2 trap in d_2-TCB at 2.0 K. Since the X-trap in neat h_2-TCB is much too dilute to obtain spin coherence signals, Shelby, Zewail, and Harris[14] used a tunable dye laser (pulsed) to measure a X-trap promotion rate constant of 53 cm^{-1} at 2.0 K. Although these measurements involved completely different experimental methods, it is clearly evident that the matrix elements for the coupling of the

trap state to the band are very sensitive to the nature of the trap. Indeed, even though the density of states in the host d_2-band is orders of magnitude less than that found in the neat h_2-TCB crystal, and also the phonon energies required for the promotion process are higher in the h_2 trap case, the h_2 trap promotion rate constant is nearly eight times larger than that of the X-trap at the same temperature.

Unfortunately, the comparison of these results may not be strictly valid since the rate constants for the thermal promotion of the h_2 trap may reflect an appreciable degree of direct trap-to-trap transfer which does not involve the exciton band.[15] This is known to be the case in the more concentrated 5% h_2 crystal.[13] Because the rates of trap-to-trap transfer tend to increase with increasing trap concentration, the thermal promotion rate constants will never show an explicit density-of-band-states dependence in the isotopic crystals. The dye laser experiments were performed only on one neat h_2-TCB crystal, therefore the dependence of the X-trap promotion rate constant on the density of band states was not established as well.[16]

A heat pulse from a source at a relatively high temperature above the bath will consist of a large number of phonons which are resonant with each of three trap depths discussed in this chapter. Thus it should be possible to induce trap delocalization in the absence of appreciable direct trap-to-trap transfer. Since the detection of heat pulse-induced trap promotion is limited only by the intensity of the trap phosphorescence, the technique is easily accomodated in both the neat h_2-TCB and the d_2-TCB systems.

Chapter III

General Theory of Heat Pulse Transmission

1. Introduction

In order to properly evaluate the experimental results obtained by the heat pulse method, one must first characterize in detail the nature of the heat pulse transmission. The frequency dependence of phonon scattering processes or the frequency-selectivity of phonon absorption processes can be studied if the spectral density of the propagating phonons is known. The crystal lattice has to behave as a transmission medium that is free of extraneous scattering centers, such that the spectral density of the artificially generated phonons remains a function of the source. This requirement usually forces the experimentalist to use very pure crystals.

Most of the experimental work since the advent of heat pulses in solids[17,18] has been done at liquid He temperatures, because the nature of the propagation becomes most interesting when the phonon mean free path approaches the crystalline dimensions. The conventional experimental arrangement for the study of heat pulse transmission requires a small resistive film which can be Joule-heated by a short current pulse, and a detector (bolometer) film which responds with a reasonable sensitivity to a rapidly changing thermal flux. In most cases, the heater film is made of constantan or nichrome, which have very low temperature coefficients of resistance. Thus the input power I^2R_H, where R_H is the resistance of the heater, is always well known and does not fluctuate with temperature. The bolometer films are often made of superconducting materials such as In or Pb, which are held at temperatures just slightly below their normal state transition temperature.[18,19] Although the superconducting devices are probably the

most sensitive , their use is restricted to temperatures in the vicinity of their transition temperatures unless fairly high magnetic fields are deployed (1 Kgauss). Another type of bolometer that is not restricted in this way is made from a semiconductor , such as germanium, which has a very steep temperature dependence for its resistivity at liquid He temperatures. [20,21] Since the crystal samples which have been normally used are hard inorganic materials, both the heater and the bolometer films are vacuum evaporated directly on to the crystal surface.

The thickness of the films (usually less than 2000 A) and their intimate thermal contact with the crystalline substrate are important features which have enabled experimentalists to obtain extremely fast (less than 10 nsec) thermal relaxation times. At liquid He temperatures, the signals produced by a heat pulse at the bolometer film will be a direct function of the transit times of the various phonon modes (one longitudinal and two transverse), provided that the input current pulse at the heater film is shorter than the transit times. The nature of the heat flow through the crystal can therefore be analyzed in terms of phonon transit times, since signals coming at times longer than that predicted by a purely rectilinear propagation are due to various scattering processes within the crystal. Thus the use of short heat pulses has focused a considerable amount of attention on two important heat transfer parameters: (1) the thermal conductivity of the crystal substrate; and (2) the thermal boundary conductance at the heater/crystal interface.

2. Thermal Conductivity of Non-Metallic Crystals

It is well known that the flow of heat within a dielectric crystal can be discussed in terms of two principal modes of phonon propagation, diffusive and ballistic. Both types of heat conduction involve a flux of phonons through the

heater/crystal interface, but the extent of phonon scattering in the crystal is what determines whether the heat flow is diffusive or ballistic. The usual expression for the thermal conductivity of a dielectric material is given by the Debye approximation

$$(8)\quad K_s = \frac{1}{3} C_s v^2 \tau \quad ,$$

where C_s is the heat capacity per unit volume, v is the velocity of sound, and τ is the mean time between scattering events of a phonon traveling with a velocity v. If the mean free path ℓ (= $v\tau$) is equal to the bulk dimensions of the crystal, then the thermal conductivity K_s is limited by the size of the crystal and the heat flow is said to be ballistic. If the mean free path of phonon propagation is much smaller than the size of the crystal, then the thermal conductivity is limited by phonon scattering and the heat flow is described as being diffusive.

There are numerous mechanisms by which phonons may be scattered, and each one has a characteristic frequency and temperature dependent relaxation time τ_i. A rigorous treatment of the relaxation time approach to the study of thermal conductivity requires solutions to the Boltzmann transport equation.[22] However, this sort of analysis goes far beyond the scope of the work presented in this thesis, since many of the authors cited are concerned with the phenomenon of second sound caused by momentum-conserving phonon-phonon interactions (N-processes). Thus for the purposes of this work, the relaxation time approximation will be discussed only in terms of resistive phonon-phonon and phonon-defect scattering processes. Since these scattering processes act together on a pulse of phonons, one would expect the individual relaxation rates τ_i^{-1} to be additive. For a flat rectangular crystal slab of thickness L, where the heat flow is primarily in

the direction parallel to the thickness, the usual form of the composite relaxation rate is given by: [23-27]

$$(9)\quad \tau^{-1} = a\nu^4 + bT^3\nu^2 + \nu/L \quad .$$

The first term refers to the defect scattering rates, where "a" is usually a constant. The second term refers to the Umklapp or resistive phonon-phonon scattering rate, where "b" is an exponential function of temperature. The third term is simply the boundary scattering rate determined by the phonon velocity and the crystal thickness L. At high temperatures, the major contribution to the relaxation rate comes from the Umklapp processes. The relaxation rate is then proportional to the phonon density and therefore to the absolute temperature. Also at high temperatures, the heat capacity is fairly constant, thus the conductivity K_s varies approximately as the inverse of the absolute temperature. However, as the ambient temperature is reduced, the number of phonons with sufficient energy to participate in Umklapp processes decreases exponentially with temperature. This results in a sharp increase in the relaxation time. Although the heat capacity begins to decrease with temperature according to the Debye T^3 law, the relaxation time increases more rapidly so as to cause an overall increase in the thermal conductivity. The thermal conductivity thus goes through a maximum (usually at about 10-20 K), and then decreases to zero with a T^3 dependence. "High" and "low" temperature ranges commonly refer to the appropriate side of the thermal conductivity maximum and the corresponding bath temperature dependences (T^{-1}, T^3). With phonon-phonon scattering effectively removed at low temperatures, the thermal conductivity is limited by the occurance of defect scattering and boundary scattering.

The first term in Eq.(9) is more precisely defined as the rate of phonon scattering at "point" defects. Point defects extend over distances in the lattice

which are much smaller than the prevailing phonon wavelengths. A defect that fits this criterion may be a wrong atom on a lattice site (such as an isotope), a vacancy at a lattice site, an interstitial atom or molecule, or a molecule that is oriented differently with respect to the translational symmetry of the lattice. Since one is actually concerned with the thermal conductivity of a molecular crystal, it would be very nice to be able to look at traps, in the light of phonon scattering, as being point defects. The quantitative analysis of phonon scattering at traps is not that straightforward, however. In the first place, there are many more isotopic species of TCB than just those associated with deuteration. Secondly, even though the concentration of the structurally defective X-trap can be estimated by the methods outlined in the previous chapter, little can be said about what the actual strain might be that leads to phonon scattering.

Isotopes will bring about a local strain at a lattice site due to the change in mass of the molecule. Walter and Pohl [27] found that the total isotopic scattering rate can be expressed as

$$(10)\quad \tau^{-1}_{iso} = (4\pi^3 V_0 S/v^3)\upsilon^4 \quad ,$$

where

$$(11)\quad S = \sum_i f_i(1 - m_i/\bar{m})^2 \quad .$$

V_0 refers to the molecular volume, v is the velocity of sound, $\bar{m}$ is the average molecular mass, and f_i is the relative concentration of mass m_i. Since the natural abundances of atomic isotopes in TCB, other than deuterium, are 75.53% Cl^{35}, 24.47% Cl^{37}, 98.89% C^{12}, and 1.11% C^{13}, one can see that there will be a large range of possible TCB masses in <u>both</u> d_2-TCB and neat h_2-TCB.[28] The actual

mass distributions for three of the TCB samples used in these experiments are shown in Table I. From Eq.(11), one can calculate the parameter S for each distribution ; the results are shown at the bottom of each column. It is evident that S does not seem to vary by more than 5% for both the protonated and perdeuterated TCB samples. In the next chapter it will be shown that the velocity of sound in TCB is roughly 1.58×10^5 cm/sec. Therefore if one assumes a 100% scattering probablity, the overall isotopic scattering rate should be approximately $4.0 \times 10^{-40} \nu^4 \text{sec}^{-1}$ in all the TCB samples.

For a typical sample thickness L = 0.03 cm, the boundary relaxation rate is about 5.3×10^6 sec^{-1}. In order for the isotopic scattering rate to be comparable to that of the boundary scattering, the phonon frequency ν must exceed 3.4×10^{11} sec^{-1}, which is equal to an energy of about 11 cm^{-1}. Thus it is possible that some of the phonons resonant with the trap depths in TCB will be isotopically scattered before they reach the boundary. If this is indeed the case, then the thermal conductivity of the TCB crystal will not be limited by the crystal size.

In general, the displacement of a molecule with respect to the surrounding molecules in a lattice will also cause a local strain. The expression for the relaxation rate due to a relative displacement $\Delta R/R$ in the molecular orientation has essentially the same form as Eq. (10), only S is replaced by $cJ^2\gamma(\Delta R/R)^2$. The term "c" is equal to the ratio of the number of defects to the number of lattice sites in the crystal. J is a constant which depends how the nearest and and further-out distances with respect to the defect combine in the scattering matrix formalism discussed by Klemens.[25] The Grüneisen constant γ appears because in a real anharmonic crystal, phonon frequencies are modified by changes in the intermolecular distance (or orientation); this is the "scattering." The complete lack of knowledge concerning the nature of the molecular displacement associated

Table I: Mass Distributions for Three TCB Samples

(AEI-MS12 Mass Spectrometer)

m_i	neat h_2-TCB f_i	0.88% hd, 0.04% h_2 in d_2-TCB f_i	1.6% hd, 5.4% h_2 in d_2-TCB f_i
214	0.3044	0.0001	0.0155
215	0.0205	0.0027	0.0055
216	0.3950	0.3126	0.3095
217	0.0266	0.0243	0.0262
218	0.1924	0.3873	0.3782
219	0.0129	0.0282	0.0282
220	0.0418	0.1848	0.1796
221	0.0028	0.0129	0.0128
222	0.0034	0.0410	0.0387
223	-	0.0027	0.0026
224	-	0.0034	0.0033
	$S = 6.4 \times 10^{-5}$	6.4×10^{-5}	6.8×10^{-5}

with the X-trap precludes any estimation of the above constants. However, since the concentration of the X-trap is so much less than practically all of the isotope concentrations listed in Table I, the effect of the local strain due to the molecular displacement would have to be enormous before scattering at this site could compete with isotopic scattering. More glaring imperfections such as those due to chemical impurities have even smaller concentrations, as evidenced by the lack of phosphorescence emission at wavelengths corresponding to the induced Y-trap. On the basis of these arguments, it will he assumed that the propagation of phonons through a thin slab of TCB at temperatures below 2.0 K will be boundary limited (ballistic), except for the possiblity of high frequency isotopic scattering.

3. Thermal Boundary Conductance Between Dissimilar Solids

The problem of heat tranafer by phonons across an interface between two dissimilar, isotropic solids at low temperatures has intrigued experimentalists and theorists for more than thirty years. Interest in the problem actually stemmed from the observation of a temperature discontinuity at solid-liquid He boundaries when heat is conducted from the solid into the He bath. The discontinuity gave rise to a thermal boundary resistance which decreased with increasing temperature approximately as T^{-3}. The phenomenon was subsequently named after its discoverer, P. L. Kapitza.[29] An extensive review on the subject of Kapitza resistances has been published by Pollack.[30] The current understanding of the Kapitza resistance is based on the large "acoustic mismatch" between a solid and liquid He. Thus the important quantities which determine the reflection and transmission coefficients of the interface are the relative densities and sound velocities of the solid and liquid He. Although the theory of the Kapitza

resistance has still not been completely solved, due to the fact that many observed values are much too low relative to the acoustic mismatch, it has been shown to be applicable to solid/solid interfaces. Much of what has been published in regard to solid/solid boundary conductances is based on an extention of the acoustic mismatch model. In particular,the following derivation of the boundary conductance is based on the work published by Little.[31]

The number of phonons of energy $h\nu$ in the heater material which strike area dA of the heater/crystal interface per unit time, at an angle of incidence between θ_H and $\theta_H + d\theta_H$, is given by

$$N_H(\nu)v_H\cos\theta_H\sin\theta_H d\theta_H dA \quad .$$

The mean velocity of the phonons (weighted average of the transverse and longitudinal modes) in the heater is given by v_H, and $N_H(\nu)$ is the product of the density of states between ν and $d\nu$ and the Planck distribution for the heater temperature T_H :

$$(12)\quad N_H(\nu)d\nu = \frac{12\pi\nu^2 d\nu}{v_H(\exp(h\nu/kT_H) - 1)} \quad .$$

Many of the phonons will be reflected and some will be refracted into the crystal at an angle between θ_B and $\theta_B + d\theta_B$. Since the two angles θ_H and θ_B can be related by Snell's law of refraction,

$$(13)\quad d\theta_B = \frac{v_B\cos\theta_H d\theta_H}{v_B\cos\theta_B} \quad ,$$

where v_B is the mean velocity of sound in the crystal, one can define a transmission factor $\alpha_H(\theta_H)$ of the interface for acoustic waves (Eq.(14)).

$$(14)\quad \alpha_H(\theta_H) = \alpha_B(\theta_B) = \left(\frac{4\rho_B v_B}{\rho_H v_H}\cdot\frac{\cos\theta_B}{\cos\theta_H}\right)\left(\frac{\rho_B v_B}{\rho_H v_H} + \frac{\cos\theta_B}{\cos\theta_H}\right)^{-2}$$

ρ_H and ρ_B are the densities of the heater and crystal materials. From Eqs.(13) and (14), the net flow of heat across the interface from the heater to the crystal, which is at temperature T_B, is given by Eq.(15):

$$(15)\quad \frac{dQ}{dt} = \iiint N_H(\nu)h\nu v_H\alpha_H(\theta_H)\cos\theta_H\sin\theta_H d\theta_H d\nu dA - \iiint N_B(\nu)h\nu v_B\alpha_B(\theta_B)\cos\theta_B\sin\theta_B d\theta_B d\nu dA \quad .$$

One can define a total transmission coefficient Γ as the integral

$$(16)\quad \Gamma = \int_0^{\pi/2} \alpha_H(\theta_H)\sin\theta_H\cos\theta_H\, d\theta_H \quad .$$

When Eq.(12) is inserted into Eq.(15), integration over all the phonons can be simplified if one makes the usual approximation that $h\nu_D/kT \to \infty$, where ν_D is the Debye cut-off frequency. Since there should be no net flow of heat across the interface when $T_H = T_B$, one can state that

$$(17)\quad \alpha_H(\theta_H)\cos\theta_H\sin\theta_H d\theta_H/v_H^2 = \alpha_B(\theta_B)\cos\theta_B\sin\theta_B d\theta_B/v_B^2 \quad .$$

The last integral of Eq.(15), which is over the total area A of the heater/crystal interface, yields the final result

$$(18)\quad \frac{dQ}{Adt} = \frac{\pi^5 k^4 \Gamma}{5v_H^2 h^3}(T_H^4 - T_B^4) = K_B(T_H^4 - T_B^4) \quad ,$$

where K_B is the thermal conductivity (ergs/sec-cm^2-K^4) of the heater/crystal interface. For a perfect acoustic match, the maximum value of the transmission coefficient Γ is unity. Most of the values reported[18,31,32] for Γ are in the vicinity of 0.5 , yielding conductivities of approximately 0.10 W/cm^2-K^4. These high values are due to the fact that the metal films are directly vacuum evaporated on to a polished crystal surface. Much lower values of the interface conductivity result if the materials are bonded or pressed together. The ramifications of the latter case will be discussed in detail in the next chapter. It should be pointed out that the acoustic mismatch model does not take into account the thickness of the heater material. Heat pulse experiments require thin metal films; however, no one has reported the observation of an explicit film thickness dependence on the value of K_B.

If $(T_H - T_B) = \Delta T << T_B$, then Eq.(18) reduces to the more familiar heat conduction equation

$$(19)\quad \frac{dQ}{Adt} \cong 4K_B T_B^3 \Delta T \quad ,$$

where T_B is the ambient or bath temperature. Under these conditions, steady-state conductivity measurements can be made if the temperature gradients in the two materials are taken into account. In heat pulse experiments involving thin films, K_B can be obtained by monitoring the exponential decay in the heater temperature following a rapid excitation with an extremely short (10 nsec) current pulse or a laser pulse:[18]

$$(20)\quad \Delta T = \Delta T_{max} \exp(-t/\tau_D) \quad .$$

When the metal films are vacuum deposited directly on the crystal, the relaxation time τ_D is equal to c_H/K_B, where c_H is the heat capacity per unit area of the thin

metal film. Eq.(20) is particularly applicable if the thermal conductivity of the crystal substrate is high enough such that there is little phonon backscattering into the metal film.[33] Since the heat capacity of the metal film is so small, the actual decay times are generally less than 10 nsec; thus these systems are ideal for producing short phonon pulses where the transverse and longitudinal can be time-resolved.

Chapter IV

Experimental Analysis of Heat Pulse Transmission in Molecular Crystals

1. Introduction

Aromatic molecular crystals such as TCB are not well-suited for supporting vacuum evaporated metal films. They have low melting points (TCB has melting point of 140°C), and they sublime very easily under vacuum. They are also very soft and fragile. Thus at the present time, the only feasible and reliable way of observing heat pulses in the crystals is to bond them to the heater and bolometer films, typically with a bonding agent like silicone vacuum grease. As was pointed out in the previous chapter, a thermal contact of this sort is usually several orders of magnitude less effective than that provided by the direct evaporation of the metal films onto the crystal.

In a steady-state measurement made by Connally, et al,[34] the thermal conductivity of a Dow silicone grease-mediated contact between a copper plate and an inorganic crystal was reported to be 3.7 $mW/cm^2\text{-}K^4$. Thus even if the inherent response time of the bolometer is very rapid, the observed bolometer signal will be greatly affected by the reduced response time of the thermal exchange process between the crystal and the bolometer and between the heater and the crystal. The problem is further compounded by the fact that a comparison of the thermal response time via the bolometer signal with that obtained more directly via the trap phosphorescence modulation can only be done with heat pulse widths in the range of 1.0 msec. The latter restriction is due to the fact that the input power dissipated in the heater film has to be kept as low as possible for the phonon absorption experiments which will be discussed later.

In order to extract the heat pulse transmission parameters from the bolometer and phosphorescence signals, the heat capacity of the sample must be known independently. There are no reported values for molecular crystal heat capacities at liquid He temperatures. Thus the first experimental results to be discussed in this chapter are the heat capacity values of TCB in the temperature range of 0.47 - 7.2 K.

2. Heat Capacity of 1,2,4,5 - Tetrachlorobenzene (TCB)

a. Experimental

A three gram single crystal of extensively zone-refined h_2-TCB was grown in a Bridgman furnace. The crystal was in the shape of a cylinder, approximately 0.7 cm in diameter and 4.5 cm long. After it was carefully weighed ($\pm$ 0.0001 gm), two thin strips of copper foil were bonded with a thick coat of G. E. 7031 varnish along the length of the sample, such that the sample was sandwiched between the copper contacts. The foils were attached with a small amount of hard, non-superconducting solder to a screw mount which was machined out of 99.9% pure copper. The entire copper unit was weighed before it was bonded to the crystal, so that the weight of the varnish could be found when the TCB-varnish-copper "sample" was weighed again. The sample was then screwed on to a tungsten rod which also supported two resistive heating elements and a precisely calibrated germanium resistance thermometer. One of the heaters actually warmed the sample rod over a specified period of time, while the other provided a constant low energy background to offset thermal losses to the surroundings. The tungsten rod was thermally isolated from a liquid ^{4}He bath by having it placed in a chamber which could be sealed with soft solder and evacuated down

to approximately 10^{-5} mm Hg. The chamber was immersed in a ^{4}He bath contained by a large cryostat located in Prof. Norman Phillips' laboratory.

Thermal contact for the tungsten rod to either the ^{4}He bath or a small adjacent chamber containing ^{3}He was effected by way of mechanical switches (clamps), which could be activated electronically. The ^{4}He bath was cooled to 1.25 K by mechanical pumping; whereas the ^{3}He bath was cooled to 0.4 K by a closed-system diffusion pump. Once the lowest bath temperatures were reached, the thermal switches were opened and the measurements were made by increasing the temperature of the isolated tungsten rod - sample assembly.

The measurement echnique, developed in Prof. Phillips' laboratory, was essentially straightforward calorimetry. The primary heating element on the rod was turned on for a pre-set period of time (usually less than 40 seconds), such that the sample-rod temperature was increased by an amount equal to roughly one-tenth of the absolute temperature prior to the heating period. Both the electrical current to the heater (0.01-0.20 μamp) and the applied voltage (0.4 - 1.2 mvolts) were carefully measured in order to calculate the amount of energy required to heat the crystal sample. The final temperature after the heating period was determined by allowing the sample temperature to drift until it no longer changed. The secondary heater offset any small thermal losses to the surroundings. The observed heat capacity of the entire sample assembly ($Q/\Delta T$) was associated with the average between the initial and final temperatures. All the contributions to the heat capacity from the tungsten rod, copper holder, varnish, and so on, were taken into account with previous data collected by Prof. Phillips and his students. A least-squares fitting program, run on a CDC 7600 computer, was used to extract the heat capacity of the TCB sample.

b. Results and Discussion

The molar heat capacity of TCB in the temperature range of 0.47 - 7.2 K is shown in Fig. (5). The best least-squares fit, given below in Eq.(21), agrees reasonably well with the Debye T^3 approximation, particularly at the lower temperatures. Due to the compounded error in all the weighings, the upper limit in the error for each value is roughly 5%.

(21) $C = 4.05T^3 - 0.0066T^5 + 9.89 \times 10^{-4}T^7$ mJ/mole-K

The Debye temperature θ_D can be calculated by using the approximation[35]

(22) $C = \frac{12\pi^4 Nk(T/\theta_D)^3}{5}$,

where N is equal to the number of molecules in the sample. If one considers the coefficient of the T^3 term in Eq.(21), one calculates a Debye temperature $\theta_D \cong 78.3$ K for the entire temperature range. From the data points in the temperature range of primary interest, 1.4 - 2.2 K, the best fit yields $\theta_D = 81.3$ K (52 cm^{-1}). The latter value of θ_D, which will be used throughout the remainder of the text, corresponds to an average phonon velocity $v = 1.58 \times 10^5$ cm/sec, calculated from Eq. (23).

(23) $$v = \frac{\theta_D k}{\hbar\left(\frac{6\pi^2 N}{V}\right)^{1/3}}$$

In Eq. (23), N is equal to the number of molecules in the sample volume V.

Unfortunately, little low temperature experimental data is reported for the elastic constants or the acoustic phonon density of states in molecular crystals. At 300 K, the time-of-flight neutron scattering spectra[36] for polycrystalline TCB indicated a density of states spectrum of lattice vibrations

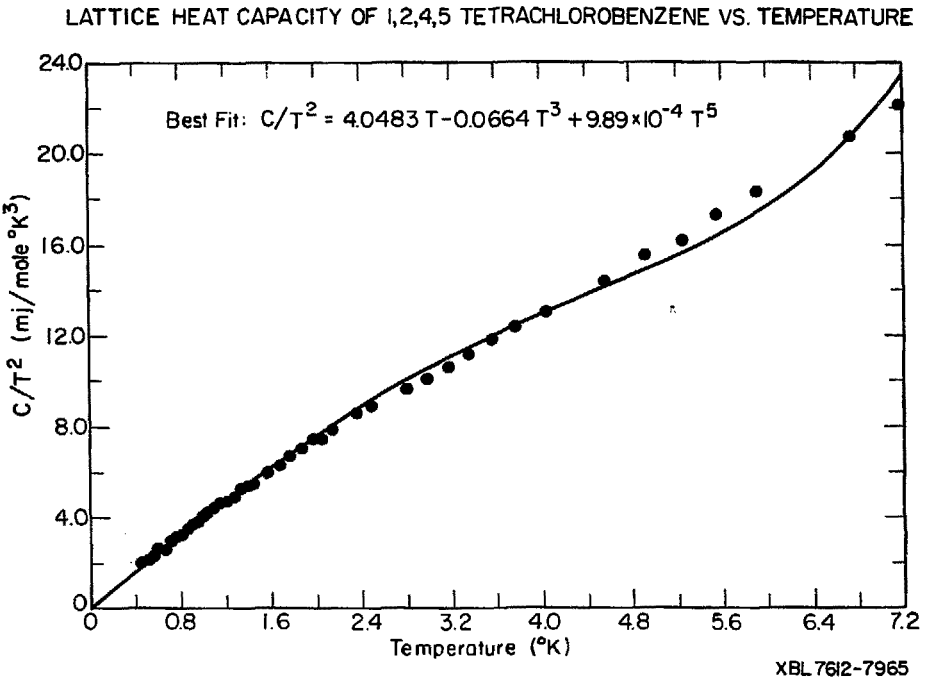

Fig. 5 The molar heat capacity of TCB. The solid line is the best least-squares fit.

between 5 cm^{-1} and 80 cm^{-1}, as well as a critical point at 52 $\pm$ 4 cm^{-1}. Model calculations have shown that the critical points observed in neutron scattering correspond to those in the phonon density of states.[37,38] Since the neutron scattering is dominated by Brillouin zone edge frequencies, the critical point at 52 cm^{-1} can be associated with the Debye cutoff for TCB. The value of θ_D calculated from the heat capacity measurements seems to correspond precisely with this critical point. For p-dichlorobenzene, the neutron scattering experiments indicated that the dispersion curves were linear up to at least 20 cm^{-1} and not markedly anisotropic.[38] Since the value of θ_D in p-dichlorobenzene from neutron scattering critical points[38] appears to be lower (40 $\pm$ 5 cm^{-1}) than that of TCB, one can assume that the dispersion curve for TCB is linear well past 20 cm^{-1}.

The higher value of θ_D for TCB may be due to a better separation of the external lattice frequencies from the internal modes. This "separation approximation" has been shown to break down significantly for the lattice vibration analysis of naphthalene (θ_D = 44 $\pm$ 6 cm^{-1}).[39-41] From the analysis of Raman active modes,[42] the lowest internal modes for p-dichlorobenzene and naphthalene are , respectively, 120 cm^{-1} and and 170 cm^{-1}; whereas the lowest internal mode for TCB is reported to be 209 cm^{-1}.[43] Thus one would expect that at higher temperatures, the excitation of the extra oscillator in TCB would be less pronounced than in the p-dichlorobenzene and naphthalene crystals. Therefore the heat capacity should not increase as significantly.

3. Bolometric Determination of the Thermal Response Time

At the beginning of this chapter it was mentioned that the thermal conductivity of a silicone grease-mediated contact was much lower than that obtained

with the direct evaporation of the heater film on the sample. Thus one is forced to measure the rise time of the bolometer signal rather than the actual pulse transit time. If the intrinsic thermal response time of the bolometer film is much shorter than that of the heater/crystal/bolometer system, then the rise time τ_R of the bolometer signal will be equal to the ratio of the crystal heat capacity to the total thermal conductance between the heater and the bolometer:

$$(24)\quad \tau_R = \frac{C}{K_{tot}} \quad \text{sec} \quad .$$

K_{tot} is the reciprocal sum of the thermal boundary conductance K_B' (mW/K) and the lattice conductance of the crystal K_s' (mW/K) :

$$(25)\quad \frac{1}{K_{tot}} = \frac{1}{K_s'} + \frac{2}{K_B'} \quad .$$

The factor of two for the second term must be there to take into account both the heater/crystal interface and the bolometer/crystal interface, which are expected to have the same thermal conductance.

The boundary conductivity ($mW/cm^2\text{-}K^4$) is hard to assess without using the approximation $\Delta T < T_B$. If one substitutes the literature[34] value of K_B, weighted by the interfacial area A and the bath temperature T_B , and the measured heat capacity values into Eqs. (24) and (25), then the determination of τ_R will give K_s' and thence the mean free path ℓ from Eq. (8) and the sample thickness. This approach assumes, of course, that the literature value was a function of the grease, and that the attenuation of the phonon transmission had little dependence on the acoustic mismatch between the materials bonded by the grease. Conversely, one could assume that the mean free path in the crystal is equal to the thickness L, since the only possible scattering processes are thought to be high frequency isotopic scattering of phonons. In this case, K_s' can be

directly calculated from Eq.(8), and K_B will be determined from the thermal rise time. In any case, it should be pointed out that the size of the crystal should be large enough to insure that its heat capacity will be larger than that of the grease and the metal films; that is, the value of C is assumed to be that of the crystal only.

a. Experimental

The thin film heater-crystal-bolometer experimental arrangement is shown in Fig.(6). A sample of extensively zone-refined TCB was cut along the principal cleavage planes (001) into a slab having a cross-sectional area of 0.06 cm^2 and a thickness of 0.025 cm. After the crystal was weighed, it was carefully bonded with silicone grease[44] to a very thin (200 Å) nichrome film which had been vacuum evaporated on to the polished end of a glass rod (3 mm diameter). On top of the crystal is a similarly bonded 1000 Å film of amorphous germanium which had been vacuum evaporated on to a 0.01 cm thick, 1.7 cm × 0.6cm, plate of glass. The crystal actually covers the entire active surface of the heater film, which was exposed a little in Fig.(6) to facilitate viewing.

The polished face of the glass rod supporting the heater film was originally cut an angle of approximately 45° with respect to the long axis of the rod, so that the same heater film could be used for the phosphorescence experiments discussed later. Before the heater film was deposited, thin strips of gold were vacuum deposited (evaporated from tungsten filaments) on to two sides of the glass rod (not shown in Fig.(6)). The rest of the rod, including the top face, was appropriately masked. After the gold was deposited, the rod was masked again such that only the top face and small sections of the gold strips near the top face were exposed. Nichrome was then evaporated from large diameter (0.060")

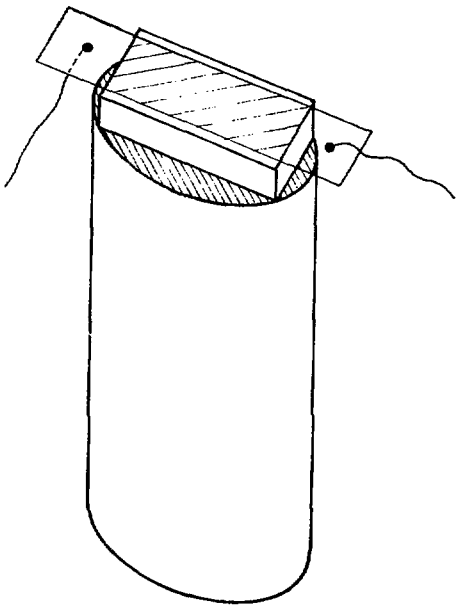

Fig. 6 The heater/crystal/bolometer assembly used to measure the thermal response time of the crystal to a 1.0 msec heat pulse. The heater (bottom) is a thin nichrome film deposited on a glass rod. The bolometer (top) is a thin germanium film deposited on a thin plate of glass. The crystal thickness (0.03 cm) is actually about the same as that of the glass substrate of the bolometer, but is enlarged here to facilitate viewing.

tungsten filaments such that a thin film was deposited on the polished face and the exposed sections of the gold strips. When 30-gauge copper wires were soldered to the lower sections of the gold strips, a complete electrical circuit to the heater film was obtained. Most of the films prepared in thia way had a resistance of 50 - 300 Ω , which could be controlled by the deposition rate. It was important that the heater film resistance be very stable with respect to temperature, in order that a constant power output was sustained when the film temperature was raised. Also the nichrome films had to be able to withstand repeated thermal cycling from liquid He temperatures to room temperature in order that the same heater film could be used over and over again to insure reproducible results in the experiments. It was found that a stable film could be obtained by heating the glass rod substrate to a temperature of 300°C, and then cleaning it with a Tesla coil-generated ionic discharge in the vacuum chamber, just prior to the nichrome evaporation. From 300 K down to 1.4 K, the change in resistance of the nichrome heater films was never more than 1%.

The germanium bolometer was manufactured in a similar manner, expect that the substrate was a flat plate of glass.[45] Electrical contact to the bolometer film was made through 30-gauge copper wires attatched to adjacent, overlapping chrome-gold contact films. When soldering to the gold films of both the heater and the bolometer, a low melting point solder (In alloy) had to be used to prevent the gold films from lifting off the substrate. At room temperature the bolometer had a resistance of around 800 Ω , for an active area of about 0.06 cm^2; but in the temperature range 1.4 - 4.2 K, the resistance changed from approximately 5100Ω to 3000 Ω. Thus the resistance was very sensitive to small temperature changes in the region of interest. A careful calibration of the resistance versus bath temperature yielded a close fit (standard deviation of

less than 1%) to the equation

$$(26)\quad R^{-1} = A\exp(-E_g/2kT) \quad ,$$

where $A = 4.16\ \Omega^{-1}$ and $E_g = 1.84 \times 10^{-4}$ eV .

The inherent response time of the bolometer supported by the glass plate was measured by immersing it in liquid He and exposing the active surface to a 10 nsec, 300 μJ laser pulse from a Molectron dye laser set at 3750 Å. A constant current source consisting of a 9 volt battery and a voltage divider was used to provide a bias of 100 μamps across the detector film. (The same bias circuit was used for the heat pulse experiments described below). The voltage changes induced by the absorption of the laser pulse were amplified by a Keithley 106 wideband amplifier and signal averaged with a Biomation 8100 transient recorder interfaced to a Northern NS-575 multichannel analyzer (CAT). The thermal response time of the bolometer to the laser pulse was 200 nsec, whereas the decay time was somewhat longer (12 μsec) due to the poor thermal conduction of the glass substrate and the surrounding He bath. The rise time of the heater film was not measured because the nichrome film resistance changes negligibly with temperature. However, when one considers the fact that the heater film is much thinner (200 Å), it would be a fairly reasonable assumption that its response time is at least as short as that of the bolometer.

The heater/crystal/bolometer system was assembled as shown in Fig. (6) and directly immersed in a liquid He bath. The ambient bath temperature was controlled by a pressure regulator in a mechanical pumping line. Monitoring of the bath temperature was made possible with the use of a calibrated germanium thermistor (Texas Instruments) located near the heater/crystal/bolometer setup. The resistances of the bolometer, heater, and thermistor were measured and checked periodically

with a Keithley 520 nanowatt dissipation bridge.

The current pulses sent through the heater film were produced by a Rutherford B-78 generator at a repetition rate of 4.5 Hz. The voltage of the pulse at the heater film was continuously checked with a Tektronix 454 oscilloscope. The rise time of the pulse was always 10 μsec or less. At a bias of 100 μamps, the bolometer voltage changes were amplified with a Keithley 104 broadband amplifier and signal averaged as described above. With a typical electrical pulse power of 0.183 W,over 1.0 msec, dissipated at the heater film, the maximum of the bolometer signal prior to amplification was on the order of 3.5 mvolts. An averaged bolometer signal obtained under these conditions is shown in Fig.(7). The spikes at the beginning and end of the detected signal are due to electrical pickup from the rising and falling edges of the applied heating pulse. The rise time for this particular pulse is about 0.45 msec, and the ambient bath temperature is 2.0 K. The maximum of the bolometer signal, ΔT_{max}, is calculated by way of the calibration curve given in Eq.(26); while the thermal rise time τ_R is calculated by convoluting a set of ten or more points with Eq.(26), and fitting the resulting values to the exponential $\Delta T_{max}(1-\exp(-t/\tau_R))$. The decay of the bolometer signal following the end of the heat pulse has a longer time constant than the rise time because of the poor thermal coupling to the surrounding He bath. The reason for the slight bump at the end of the decay is unknown at this point.

b. Results and Discussion

The experimental values of the bolometer signal rise time τ_R over the temperature range 1.48 - 2.14 K are shown in Fig.(8). At each temperature, the input pulse power to the heater was 1.21 W, which,over a interface area of 6 mm^2,

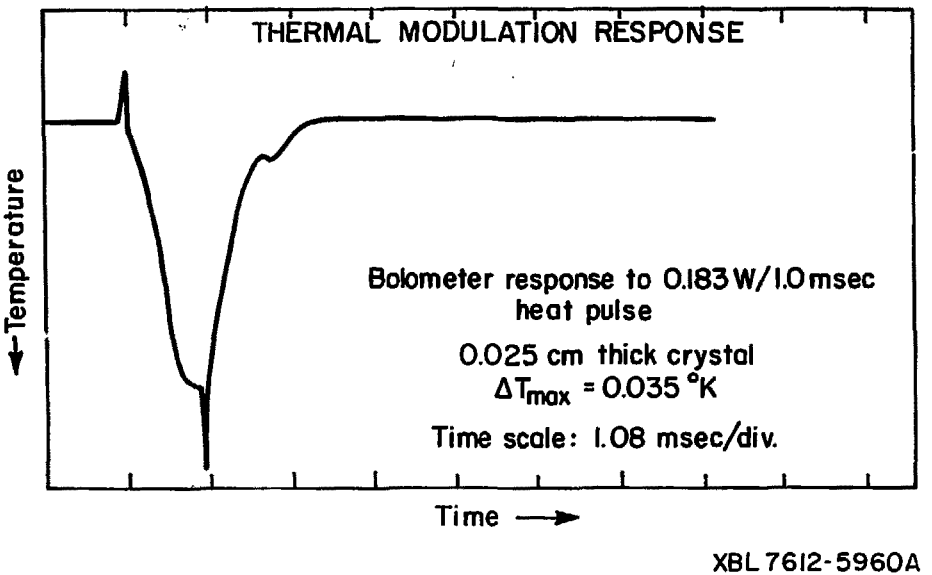

Fig. 7 Signal-averaged bolometer response to a 1.0 msec heat pulse. The negative voltage change is converted into a positive temperature change above the 2.0 K bath temp.

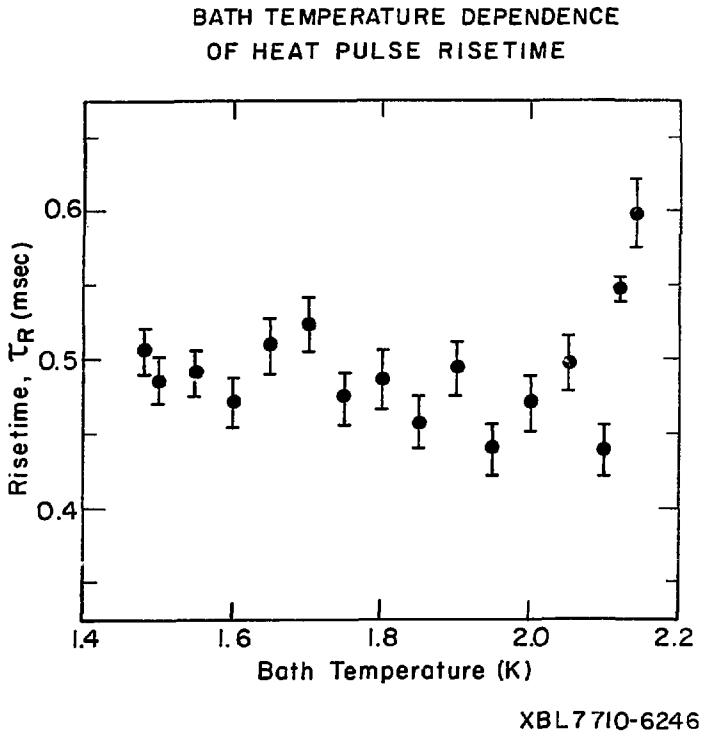

Fig. 8 The rise times of the heat pulse in the heater/crystal/bolometer system for 0.20 W/mm^2, 1.0 msec heat pulses at various bath temperatures. The error bars refer to the goodness of the fit to an exponential rise in lattice temperature. The sudden rise in τ_R near 2.15 K is a liquid He effect.

is equivalent to 0.20 W/mm . The high values of τ_R are clearly not due to the response time of the bolometer; instead, the bolometer is following the crystal temperature. Since both the thermal conductance K_{tot} and the heat capacity C in Eq.(24) are expected to vary as T^3, there should be no temperature dependence for τ_R. One can see from the data that this is roughly the case, except for the sudden rise in τ_R near the lambda point (2.17 K) of the liquid He.

If one chooses the second approach in the data analysis mentioned at the beginning of this section, one then proceeds to calculate the boundary conductivity K_B by assuming that the conductivity of the crystal is limited by the crystalline dimensions. The results of these calculations, based on the values of τ_R and C, are shown in Fig.(9). The conductivity K_B is clearly close enough to the literature value [34] of 3.7 T^3 mW/cm^2-K to verify the premise that the phonon mean free path in the crystal is indeed limited only by the crystal thickness. Since the bolometer results are very similar to the cited literature value, one can also conclude that the grease is the primary source of attenuation at the heater/crystal or crystal/bolometer interface.

If the acoustic mismatch model is applicable to a composite system such as the heater/grease/crystal interface, then one could calculate an "effective" overall phonon transmission coefficient Γ from the results presented here. Since K_B = 3.4 mW/cm^2-K^4, and the velocity of sound in the nichrome film[46] is about 3.4×10^5 cm/sec, then Γ = 0.07. However, another important experimental feature, which has been ignored in the discussion so far, is the fact that the entire system had been immersed in liquid He below the lambda point. Because of the tendency of superfluid He to penetrate materials and crevices with uncanny ease,[47] one could assume that the grease interface is imbued with it. The value of Γ for solid/liquid He boundaries [30] is generally about 0.005, due to the low

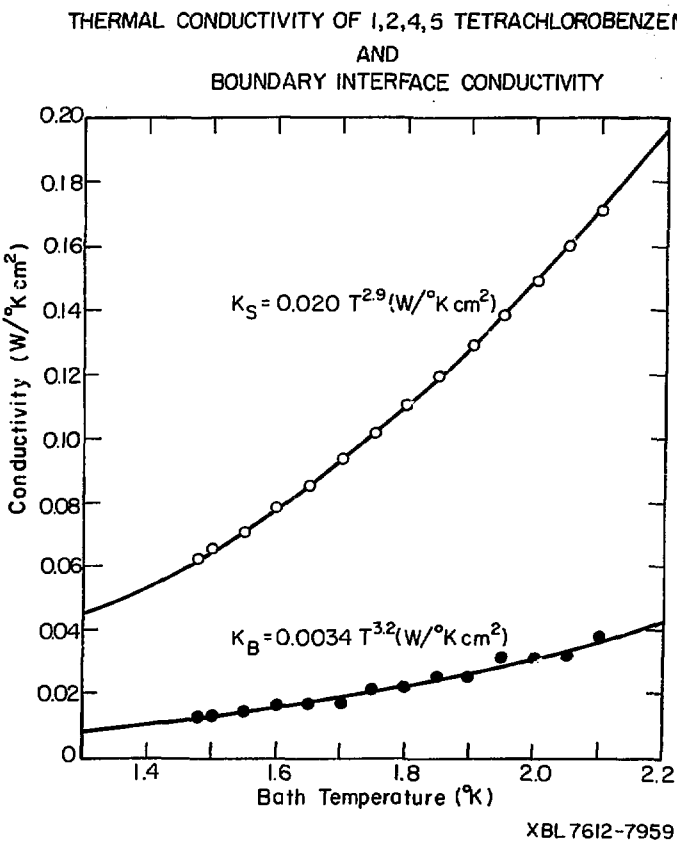

Fig. 9 From the heat capacity values of a 0.025 cm thick crystal having a cross-sectional area of 0.06 cm^2, the thermal conductivity K_s (white points) of the crystal is calculated. The mean free path of the phonons in the crystal is equal to the sample thickness. The heater/crystal boundary conductivity K_B is calculated from K_s and the rise time τ_R. The curves are the best fits for the data points.

density and slow velocity of sound in liquid He. Thus there may be an additional contribution to the overall impedance of the heater/crystal/bolometer system from the liquid He. The sharp rise in the thermal response time τ_R when the bath temperature is near the lambda point is probably a manifestation of this contribution, since the velocity of sound in liquid He is attenuated even more at temperatures within 0.01 K of the lambda point.[48] A similar behavior is observed in the phonon bottleneck experiments reported by Glättli,[49] where it was found that the spin relaxation time suddenly increased near the lambda point. Buckley and Francis[50] also noticed this effect in their study of microwave - generated phonon propagation in durene.

4. Heat Pulse Transmission and Trap Phosphorescence Decay

a. Experimental

Highly purified h_2-TCB was prepared by zone-refining through 1400 or more passes re-crystallized, reagent grade material. No sign of chemical impurities (e.g. Y-traps), showed up in the phosphorescence spectrum, and strong exciton emission was observed at temperatures as low as 2.0 K. The d_2-TCB was synthesized by the Fooladi method.[51] On two separate occasions,[52] perdeuteration was 98.6% (1.16% hd and 0.23% h_2) and 99.1% (0.88% hd and 0.04% h_2). Following deuteration, the material was zone-refined. Higher concentrations of h_2-TCB were incorporated by adding small amounts to the d_2-TCB material just before the crystals were grown. Each crystal was grown from the melt in a Bridgman furnace[53], and later annealed for ten days at 138°C.

The hd and h_2- TCB concentrations for all the d_2-TCB samples were determined by an oscillograph analysis of the mass spectrum taken with an AEI-MS12 spectrometer run at 12 eV. The intensities of each peak were measured by hand and

normalized with respect to the total of all the peak intensities (see Table I for some examples). Each normalized peak intensity could be fit to the equation below, where c(x) refers to the percent concentration of the species x-TCB.

$$(27a)\quad I_{m_i} = c(h_2)P_{m_i}(h_2) + c(hd)P_{m_i}(hd) + c(d_2)P_{m_i}(d_2)$$

$$(27b)\quad \sum_i \left(P_{m_i}(h_2) + P_{m_i}(hd) + P_{m_i}(d_2) \right) = 1$$

The value $P_{m_i}(x)$ is equal to the probability of a mass m_i being associated with an x-TCB molecule. As was mentioned earlier in Chapter III, these probabilities can be calculated from the natural abundances of the Cl and C isotopes.

Just as in the bolometer experiment, each neat h_2-TCB and d_2-TCB sample was cut from a single crystal along the principal cleavage planes (001) into a slab having a cross-sectional area of 0.06 cm^2 and typical thickness of 0.025 - 0.05 cm. Prior to the experiment, the sample was carefully weighed in order to ascertain the thickness and the heat capacity. The sample was then bonded with a very thin layer of silicone grease to the same heater film used in the bolometer experiment. The crystal/heater assembly was inserted into the same cryostat and was totally immersed in liquid He. The temperature of the bath was controlled and monitored as before.

The experimental arrangement is shown in Fig.(10). Each sample was excited into the upper singlet state manifold by a PEK 100W high pressure Hg arc lamp filtered at 2800 Å. The subsequent phosphorescence from the lowest vibrational level of the first excited triplet state T_1 was detected at 90^0 with a 3/4 meter Jarrel-Ash Czerny-Turner monochromator, equipped with an EMI 6256S photomultiplier. The emission from the X-trap in neat h_2-TCB and the emission from the hd and h_2-TCB traps in d_2-TCB were easily resolved with res-

THIN FILM GEOMETRY

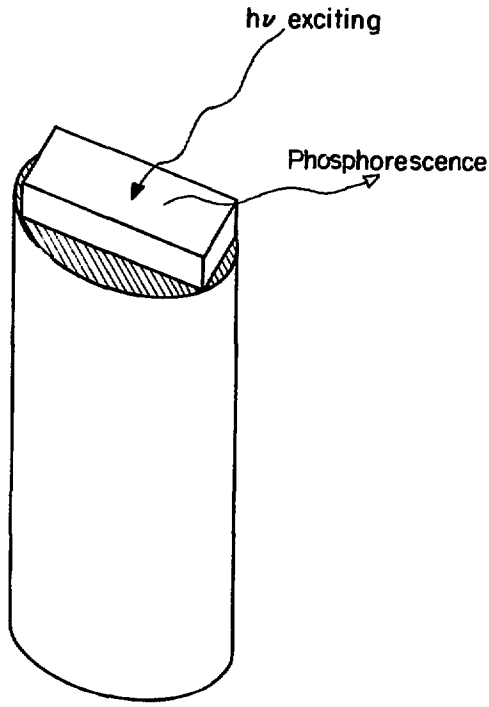

XBL 7612-7961B

Fig. 10 Heater/crystal arrangement for the optical detection of trap phosphorescence changes due to heat pulse propagation. The emission from the surface of the crystal is detected at 90° from the exciting light. The heater is the same thin film used in the bolometer experiments.

pect to the exciton lines. By using a slit width of 10 μ or less, the spectroscopic trap depths Δ were determined after the calibration of the grating drive with a low pressure neon lamp. In each case, the spectrum was recorded on a strip chart from the output of a Keithley 610CR electrometer interfaced to the cooled photomultiplier. The temperature dependence of the phosphorescence intensity was determined by scanning the trap regions repeatedly at various bath temperatures; care was taken to maintain the settings on the electrometer and the slit width for a given temperature dependence. The X-trap data points were fit with the parameters in Eq.(5) by a computer program which normalized the phosphorescence intensities in such a way as to yield the best-fit for a given set of 4ß, Δ, and n values.

The heat pulse-induced phosphorescence modulation experiments were carried out as follows. The grating of the monochromator was set at the peak of the trap (or exciton) emission; the slit width was then increased to 50μ - 100 μ to increase the light intensity. The output of the photomultiplier was sent to the Northern CAT used earlier in the bolometer experiment. An electronic shutter was placed in front of the monochromator entrance slits so that the dark level of the photomultiplier could be established. The shutter was triggered to open for $1/15^{th}$ second at a repetition rate of 4.5 Hz. After a delay time suitable to establish the level of the steady state phosphorescence intensity I_{ss} (i.e., when the shutter was completely open), a 1.0 msec current pulse from the Rutherford generator was dissipated at the heater film. The resulting signal, shown in Fig.(11), was averaged 512 times or more on the CAT. Thus each signal is composed of the dark level, the I_{ss} level, and the heat pulse modulation ΔI_{max}. In the case of trap modulation, ΔI_{max} is a negative change in light intensity; whereas, in the case of exciton modulation, ΔI_{max} is a positive

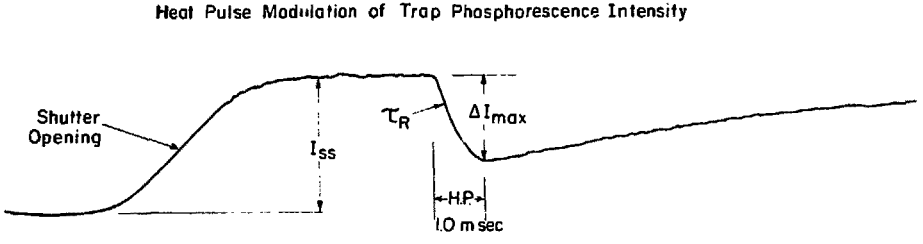

Fig. 11 Time-resolved heat pulse modulation of trap phosphorescence intensity obtained by signal averaging. The steady-state emission intensity I_{ss} is established by opening a shutter which is in front of a monochromator. The modulation depth ΔI_{max} always coincides with the end of the heat pulse.

change. All the pulse voltages across the heater film were monitored on the Tektronix 454 oscilloscope. The shutter, Rutherford, and CAT were triggered by separate pulses from a General Radio modular pulse generator (Type 1395-A), in order that appropriate trigger delays were obtained.

The rise time τ_R of the phosphorescence modulation was calculated by fitting a set of ten or more points to the expression $\Delta I = \Delta I_{max} (1 - \exp(-t/\tau_R))$. The modulation depth ΔI_{max} always coincided with the end of the heat pulse. In Fig. (11), the slow return back to the steady-state level, following the end of the heat pulse, is due primarily to the long radiative lifetime of the triplet state[6] and the slow trapping rate.

b. Results and Discussion

There are several important aspects in the analysis of the trap phosphorescence response time τ_R; thus the discussion will be restricted at first to the single trap case of the X-trap in neat h_2-TCB. One will want to compare the values of τ_R with those obtained with the bolometer. Then a discussion of the dependence of K_B on the type of grease will be presented. Finally, the possibility of a contribution to the phosphorescence response time from spin-lattice relaxation processes among the triplet sublevels will be discussed.

In the bolometer experiments, the heat pulse was required to propagate through the sample in order to be detected. Since most of the phosphorescence emitted by the crystal comes from the molecules near the surface exposed to the exciting light, the heat pulse is again required to propagate through the crystal before it is detected. Therefore, the rise time of the phosphorescence modulation should also be a function of the sample heat capacity and the total thermal conductance to the crystal surface exposed to the exciting light. The only differ-

ence will be that the factor of two will be removed from Eq.(25), since one does not have to take account of a crystal/bolometer conductance.

The results shown in Table II were obtained by maintaining a constant bath temperature (e.g. 2.00 K), and averaging the values of τ_R over a typical input power range of 0.05 - 0.20 W/mm^2 . The heat capacity values were calculated from Eq.(21). One can see that τ_R is definitely a function of C and the thermal boundary conductance. However, if the values of the conductance K_B' are normalized with respect to the bath temperature and the common interfacial area of 6 mm^2, the resulting values of the conductivity K_B are higher than that found in the bolometer experiment. This feature is also observed in the bath temperature dependence of τ_R for sample A (not shown in Table II), where $K_B = 4.88T^{2.9}$mW/cm^2-K^4 for a constant power input of 0.20 W/mm^2.

There are many possible reasons for this discrepancy. The approximation $\Delta T < T_B$ may not really be valid for the heater/crystal interface conductivity. In the bolometer experiments, the crystal/bolometer interface is removed far enough away from the heater for $\Delta T < T_B$ to be valid, but perhaps the value of K_B should not have been taken as the average of the two interfaces. Also, the absence of the bolometer in the phosphorescence experiments probably provides for a much better thermal coupling to the He bath. Although the crystal/bolometer conductance is expected to be much higher than the crystal/liquid-He conductance, it is entirely possible that this assumption is not true. In many cases it has been shown that the solid/liquid-He conductances for high frequency phonons (10^{11}Hz) are much higher than that predicted by the acoustic mismatch theory.[54-56] Thus if the phonons are allowed to escape from the crystal surface at a rate which is much faster than the rate at which they enter the crystal at the heater interface, the conductance at the heater interface will actually seem higher, due to

Table II: Heat pulse transmission parameters, X-trap in h_2-TCB

Sample	T_B (K)	Thickness (cm)	C ± 5% (μJ/K)	τ_R (msec)	K_B' (mW/K)	K_B (mW/cm^2-K^4)
A	2.00	0.080	1.259	0.449 ± 0.101	2.90 ± 0.94	6.03 ± 1.96
B†	2.00	0.039	0.605	0.186 ± 0.050	3.86 ± 1.42	8.04 ± 2.97
C	2.00	0.050	0.787	0.260 ± 0.037	3.32 ± 0.80	6.91 ± 1.68
C*	2.00	0.050	0.787	0.263 ± 0.040	3.28 ± 0.83	6.83 ± 1.72
C	1.75	0.050	0.535	0.271 ± 0.059	2.16 ± 0.68	6.70 ± 2.13
C*	1.75	0.050	0.535	0.282 ± 0.067	2.06 ± 0.70	6.42 ± 2.17
C	1.48	0.050	0.328	0.211 ± 0.036	1.74 ± 0.47	8.96 ± 2.43
C*	1.48	0.050	0.328	0.234 ± 0.055	1.55 ± 0.52	7.98 ± 2.68

† Apiezon N grease

* b_{2g} emission

less backscattering.

Despite the fact that the K_B values cannot be determined very precisely, it is still evident that the thermal conductance of the crystal is limited by the crystal size. Further support for this conclusion lies in the fact that the rise time τ_R was not a function of the input power. If scattering processes in the crystal were limiting the conductance, then one would expect phonon-phonon scattering rates to increase with the increasing flux densities at higher heat pulse powers. Furthermore,at higher heat pulse powers, there is a greater density of high frequency phonons, which are more likely to scatter at point defects ($\ell^{-1} \propto \nu^4$). Thus the lack of a τ_R power dependence seems to indicate that the phonon mean free path ℓ in the crystal is not limited by bulk scattering processes.

Connally, et. al., also reported [34] that the analogous thermal conductivity for an Apiezon N grease mediated contact is six times higher than that for silicone grease. This could be explained by a possible difference in the bulk conductivities of the grease. The grease mediated heater/crystal interface would then be viewed as a complicated composite boundary problem, as shown in Fig.(12). The true acoustic mismatch conductivities of the heater/grease and the grease/crystal material boundaries are K_{HG} and K_{GS}; and the bulk thermal conductivity of the grease is given by K_G. The composite heater/crystal conductance would then be

$$(28)\quad \frac{1}{K_B'} = \left(\frac{A}{K_{HG}} + \frac{A}{K_{GS}} + \frac{d}{AK_G} \right) \text{ K/mW} \quad ,$$

where A is the interfacial area and d is the thickness of the grease.

A quantitative analysis of K_B' in Eq.(28) would require an accurate estimate of the grease thickness. This was not done in these experiments. However, all the

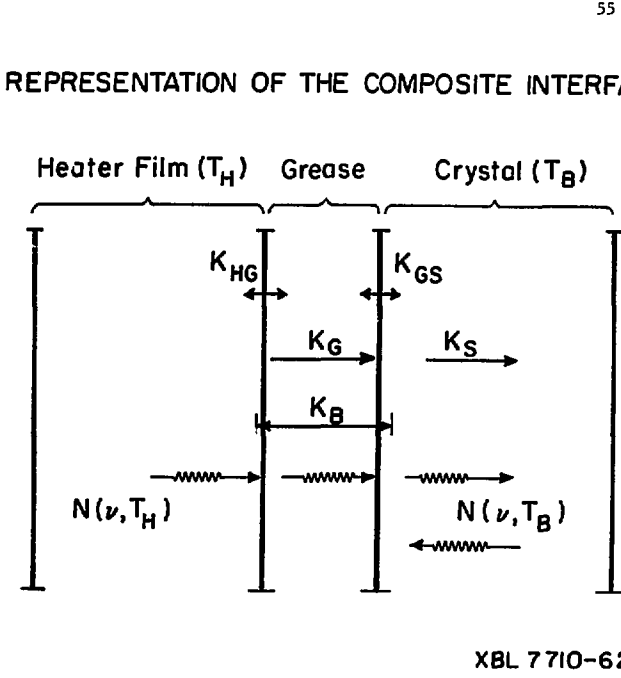

Fig. 12 The heater/crystal interface may be viewed as a composite thermal conduction problem consisting of three dissimilar materials and two boundaries. The overall conductivity from the heater to the crystal is given by K_B. The bulk thermal conductivity of the grease is K_G, while that for the crystal is K_S. The values of K_{HG} and K_{GS} would be the "true" boundary conductivities. The net flux of phonons of frequency ν from the heater at temperature T_H to the crystal at temperature T_B is equal to $N(\nu,T_H) - N(\nu, T_B)$.

runs that used silicone grease, including those in Table II, had values of K_B' that were reproducible to within 50 %. Apiezon N grease was used for sample B in Table II, and one can see that the resulting boundary conductance is somewhat higher than that given for samples A and C. However, it is definitely not as high as that found by Connally, et. al.. Thus either the grease thickness was significantly different from all the silicone grease runs, or there really is not a dependence on the bulk conductivity of the grease for very thin coverages.

The response time of the corresponding exciton modulation is roughly the same as that observed for the X-trap. The relative modulation depth $\Delta I_{max}/I_{ss}$ of the exciton phosphorescence also quantitatively matched the modulation depth of the X-trap. This situation occured only at relatively low heat pulse powers (< 0.20 W/mm). At higher powers, the exciton population is suddenly depleted by exciton triplet-triplet annihilation[7]. The rate at which the annihilation occurs is proportional to the square of the exciton population created in the band by the heat pulse. Thus the shape of the phosporescence modulation distorts in comparison to that of the X-trap at high powers. As long as the power is kept reasonably low, the exciton modulation indicates that the X-trap changes are due to heat pulse-induced promotion to the band.

Another way to check to see if indeed the X-trap phosphorescence modulation is only due to thermal promotion is to look for spin-lattice relaxation among the sublevels of the triplet trap state. In zero field[8], the three sublevels are separated by approximately 0.10 cm^{-1}, and are characterized by a non-Boltzmann population distribution under steady-state excitation conditions. Thus a convenient way of determining the extent of spin-lattice relaxation is to compare the rise time and modulation depth of the phosphorescence emission from two of the sublevels. The τ_y sublevel radiates primarily to the origin (a_g) at 3751 Å,

while the τ_z sublevel radiates primarily to the b_{2g} vibrational mode of the ground state at 3784 Å. This situation is depicted in Fig. (13) for the case where h_2-TCB is a trap in durene. Although the emission wavelengths are slightly different, the analysis is the same.

The h_2-TCB trap is roughly 1400 cm^{-1} below the durene host band, thus no thermal promotion processes are possible at cryogenic temperatures. However, due to the non-Boltzmann spin distribution, the phosphorescence intensity can be modulated either by irradiation of the sample with microwaves which couple only two of the sublevels, or by a heat pulse which equalizes all three of the sublevel populations. Both spectra in Fig.(13) were obtained by way of phase-sensitive detection (PAR lock-in amplifier). The phosphorescence changes are slightly different in the two experiments because the microwave power was below the level of saturation, whereas the heat pulse saturates the the sublevels via spin-lattice relaxation. One can see that for the triplet state of TCB in durene, where the population in τ_y is less than the population in τ_z, the heat pulse will cause a net increase in the phosphorescence intensity to the origin and a net decrease in the intensity to the b_{2g} level of the ground state.

Both the τ_y and τ_z sublevels have radiative lifetimes which are much shorter (38 msec) than the "dark" τ_x sublevel (370 msec). If the exciting light is abruptly turned off (shuttered), then the phosphorescence intensity at the origin and the b_{2g} wavelengths will decay at a rate equal to the τ_y and τ_z reciprocal lifetimes, respectively. However, if a heat pulse is triggered at various delay times after the shutter is closed, a jump in the phosphorescence intensity at either the origin or the b_{2g} level is observed. Thus the empty τ_y and τ_z sublevels experience a sudden increase in population. The

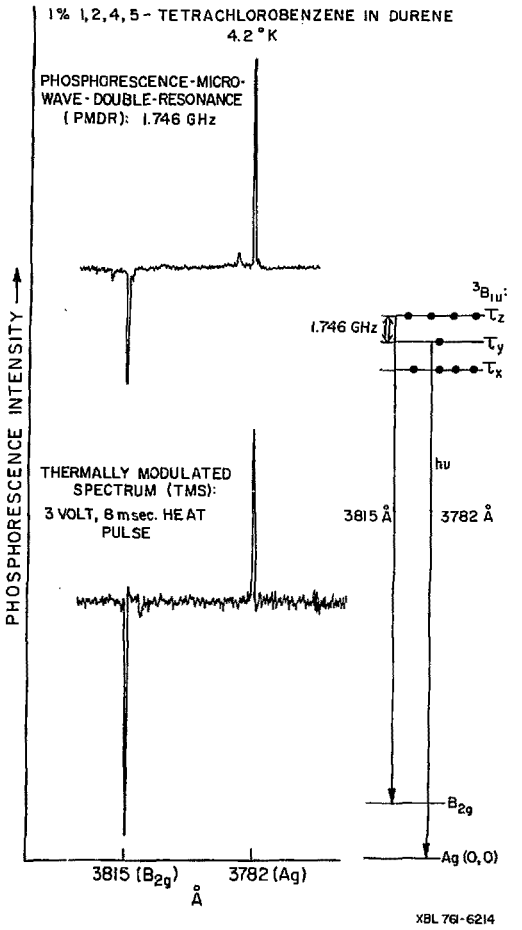

Fig. 13 Phase-detected phosphorescence modulation spectra obtained with microwave coupling of two triplet sublevels (upper) and heat pulse equilibration of all three sublevels (lower). In this crystal, TCB is a very deep trap (1436 cm^{-1}) in a durene host lattice; thus the heat pulse phosphorescence modulation is due only to spin-lattice relaxation.

height of the jump at the various delay times is proportional to the population remaining in the τ_x sublevel. If one plots the logarithm of the height for the phosphoresence jump versus the heat pulse delay time, the slope yields a rate constant which is equal to the reciprocal lifetime of the τ_x sublevel. This can be seen in Fig.(14).

It is clear then that a heat pulse will induce spin-lattice relaxation processes among the triplet sublevels in such a way as to bring about phosphorescence changes. Since thermal promotion of the trap state to the level of the exciton band is also detected by way of phosphorescence changes, one has to show that these changes are due only to the delocalization processes and not spin-lattice relaxation as well. For the 17 cm^{-1} X-trap, $\tau_y > \tau_z$.[11] Thus if there is any net transfer of population from τ_y to τ_z during the course of the heat pulse, then the rise time of the phosphorescence modulation detected at the origin should be faster, and the relative modulation depth $\Delta I_{max}/ I_{ss}$ should be greater, than the corresponding values for the emission detected at the b_{2g} level. This was never observed. All the data for the X-trap phosphorescence modulation experiments indicate that the values of τ_R and $\Delta I_{max}/I_{ss}$ are independent of which sublevel was monitored. Therefore, one can conclude that the decrease in the phosphorescence intensity is due exclusively to delocalization.

In Tables III and IV, the results are shown for the phosphorescence modulation response times of the hd and h_2 traps in d_2-TCB. Ideally, they should yield identical response times, relative to the crystal size, as that found for the X-trap. It is evident, however, that the response times τ_R are longer, even though the samples were thinner. The longer τ_R values result in proportionately lower K_B' values. (It should be noted that the heat capacity of d_2-TCB is not expected to be significantly different from that of h_2-TCB; thus Eq.(21) is used

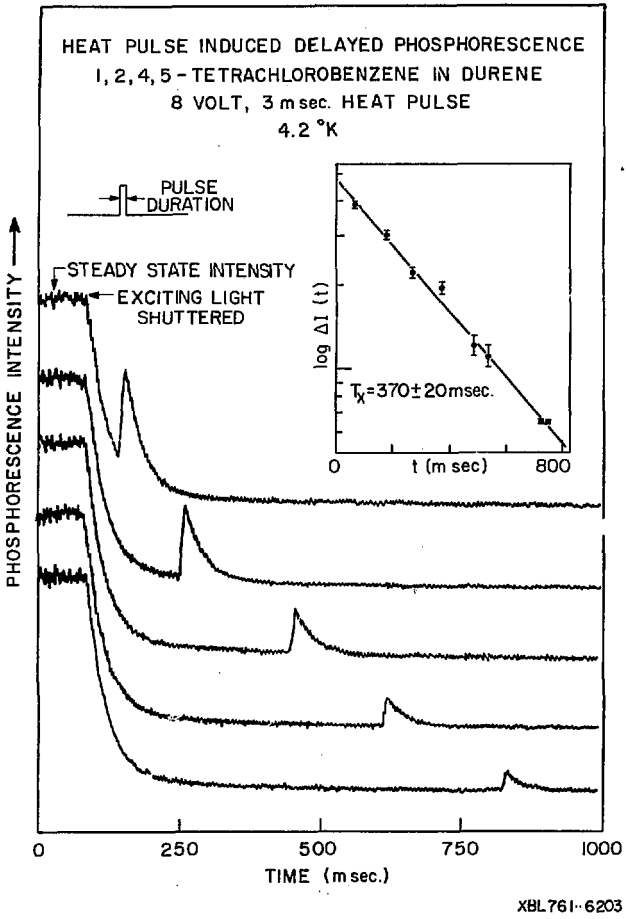

Fig. 14 Heat pulse induced delayed phosphorescence changes (increases) monitored at the electronic origin (τ_y emission) of the TCB trap in durene. When the pulse delay time is accurately known, the lifetime of the "dark" τ_x sublevel can be obtained (inset).

to calculate C.) As was pointed out in Chapter III, the isotopic scattering rate in the bulk of the d_2-TCB crystals should not differ from that in neat h_2-TCB by more than 5%; the longer τ_R values thus cannot be attributed to isotope scattering alone. It is also clear from these results that there is no phonon frequency dependence in the boundary conductivity, since the depth of the X-trap is in between that of the hd and h_2 trap depths. Using the method just outlined above, the author found no indication that spin-lattice relaxation processes were the cause of this discrepancy.

The only plausible explanation at this time is that there must be a net transfer of triplet population from one trap to the other during the course of the heat pulse. This is much less likely to happen in the neat h_2-TCB crystals because the X-traps are separated by more than 10^4 host molecules (it would be impossible to see anyway for a single trap system). However, in the d_2-TCB system there are two distinct traps that are separated on the average by never more than 110 host molecules in the most dilute crystal (0.88% hd, 0.04% h_2). If energy transfer is occuring, then either the exciton migration in the band is not completely interrupted by the presence of the heat pulse flux, or direct trap-to-trap transfer is effective even in the dilute crystals.(Both processes may be happening at the same time, of course). From the data presented in Tables III and IV, one observes that the hd trap response times in the dilute crystals (samples D, E, and F) are slower than the corresponding h_2 trap response times. Although it is not shown in the tables, the hd trap response times actually increase slightly with increasing power, whereas the h_2 trap response times decrease slightly with increasing input power. At high input powers (0.20 W/mm^2), the h_2 trap response times approach values which are equivalent to those found for the X-trap (relative to the crystal size). Thus it appears that energy is being

Table III: Heat pulse transmission parameters, hd trap in d_2-TB

Sample	Trap Conc.	T_B (K)	Thickness (cm)	C ± 5% (μJ/K)	τ_R (msec)	K_B' (mW/K)	K_B (mW/cm^2-K^4)
D	1.16%hd, 0.23% h_2	2.00	0.024	0.377	0.407 ± 0.063	1.05 ± 0.27	2.19 ± 0.56
E	0.88%hd, 0.04% h_2	1.70	0.027	0.261	0.309 ± 0.013	0.98 ± 0.14	3.32 ± 0.47
E	"	1.45	0.027	0.164	0.236 ± 0.032	0.65 ± 0.13	3.53 ± 0.74
F	"	1.50	0.024	0.163	0.301 ± 0.072	0.64 ± 0.72	3.18 ± 1.08

Table IV: Heat pulse transmission parameters, h_2-trap in d_2-TCB

Sample	Trap Conc.	T_B (K)	Thickness (cm)	C ± 5% (μJ/K)	τ_R (msec)	K_B' (mW/K)	K_B (mW/cm^2-K^4)
D	1.16% hd, 0.23% h_2	2.0	0.024	0.377	0.336 ± 0.045	1.31 ± 0.31	2.72 ± 0.64
D	"	1.70	0.024	0.235	0.213 ± 0.032	1.42 ± 0.36	4.82 ± 1.21
E	0.88% hd, 0.04% h_2	1.80	0.027	0.309	0.229 ± 0.082	1.65 ± 0.76	4.73 ± 2.17
E	"	1.70	0.027	0.261	0.245 ± 0.038	1.29 ± 0.33	4.37 ± 1.11
E	"	2.0	0.027	0.418	0.262 ± 0.027	1.90 ± 0.39	3.96 ± 0.80
G	1.42% hd, 0.78% h_2	1.50	0.026	0.175	0.341 ± 0.035	0.59 ± 0.12	2.91 ± 0.59
G	"	2.00	0.026	0.404	0.348 ± 0.028	1.33 ± 0.24	2.77 ± 0.50
H	1.6% hd, 5.4% h_2	2.00	0.031	0.489	0.356 ± 0.030	1.53 ± 0.28	3.19 ± 0.59
H	"	1.50	0.031	0.212	0.334 ± 0.052	0.71 ± 0.18	3.52 ± 0.90

transferred from the deep h_2 trap to the shallow hd trap,at least when the heat pulse power is relatively high. At relatively low powers (< 0.10 W/mm^2), one might expect to see a transfer of energy from the shallow to the deep trap; this has been observed only a few times.

5. Concluding Remarks

In this chapter, the author has endeavored to show that the thermal response of a thin molecular crystal slab bonded to a heater film is governed by the conductance of the heater/crystal interface and the lattice heat capacity. Given the fact that the thermal conductivity of the heater/crystal interface is roughly the same as that measured by other workers for similar thermal contacts, it appears that the initial assumption of a sample thickness-limited phonon mean free path in the crystal is correct. Thus the flow of heat in the crystal is ballistic in nature, while the heater/crystal interface has a relatively low phonon transmission coefficient.

The optically-detected time response of the single X-trap system in neat h_2-TCB was comparable with the thermally-detected response times obtained with the bolometer. Thus the rate of depletion of the X-trap population is limited by the rate at which the resonant phonons enter the crystal. This is an important conclusion because one can now begin to characterize the spectrum of the phonon pulse in terms of the frequency distribution entering the crystal at the heater interface. The quantitative analysis of the relative modulation depth $\Delta I_{max}/I_{ss}$ will be particularly applicable to traps that are close in energy to the exciton band, for the rate of thermal promotion to the band greatly exceeds the rate of spin-lattice relaxation among the sublevels.

Although the phosphorescence modulation response times in the isotopic

crystals seem to be affected by what is thought to be energy transfer processes among the traps, the trap populations are also depleted in the same fashion as that observed for the single X-trap system. There does not seem to be a clear-cut dependence of τ_R on the relative trap concentrations in the d_2-TCB crystals, even when the h_2 concentration is increased from 0.23% to 5.4%. Unfortunately, one cannot check this observation for the h_2 trap response times with the corresponding hd response times, because all the excitation resides in the deeper h_2 trap in the concentrated crystals. Despite the problem of energy transfer processes , the multiple trap system is well-suited to analyze the spectrum of the phonon pulse. The presence of two frequency-selective phonon absorption centers in the crystal will allow one to correlate the resonant phonon frequencies to a common source spectrum.

Chapter V

Phonon Spectroscopy

1. Introduction

It was shown in Chapter III that the energy lost per unit time from the heater film was proportional to the thermal conductance away from the film and the fourth power of the film temperature. One may rewrite Eq.(18) in terms of the total acoustic power per unit area:

$$(29)\quad \frac{P(T_H,T_B)}{A} = \frac{\pi^5 k^4 \Gamma (T_H^4 - T_B^4)}{5 v_H^2 h^3} \quad .$$

This relationship is completely analogous to the Stefan-Boltzmann law for the thermal radiation of photons, where $\frac{\pi^5 k^4 \Gamma}{5 v_H^2 h^3}$ is equivalent to the Stefan-Boltzmann constant. In fact, since the velocity of sound v_H is smaller than the velocity of light by a factor of 10^5, the thermal emission of phonons is a factor of 10^{10} more efficient. The transmission coefficient Γ takes on the connotation of a "spectral emissivity" [57,58] of the interfacial area. Thus when Γ is the maximum value of 1.0 under ideal acoustic matching conditions, the heater is a perfect black body radiator of phonons. If the phonon transmission medium is relatively free of extraneous scattering centers, then all studies analogous to those made with optical spectrometers on electromagnetic radiation can be made on acoustic phonon radiation: frequency dependence of emissivity, scattering, absorption, etc.. In particular, it would be useful to determine the phonon absorption coefficient for the process of trap state delocalization as a function of the density of available band states and the nature of the trap.

2. Heaters as Broad-Band Phonon Sources

From the acoustic mismatch theory of Little[31] and Weis[57], it can be shown that the net flux of phonons of all polarizations with frequency ν from the heater at a temperature T_H is given by:

$$(30)\quad N(\nu,T_H,T_B) = \frac{6\pi A\Gamma\nu^2}{v_H^2}\left[\frac{1}{\exp(h\nu/kT_H) - 1} - \frac{1}{\exp(h\nu/kT_B) - 1}\right] .$$

Several curves of $N(\nu,T_H,T_B)$ versus ν for various heater temperatures T_H are shown in Fig.(15), where the bath temperature T_B is 2.0 K. (The vertical dotted line is the 52 cm^{-1} Debye cutoff for TCB. The effect of dispersion near the cutoff is neglected). It is evident that the spectrum of the phonon flux displays a maximum which shifts to higher frequencies with increasing heater temperature. The linear relationship between the maximal frequency ν_{max} and T_H is analogous to the well-known displacement law

$$(31)\quad \nu_{max} \cong \frac{2kT_H}{h} .$$

Many of the initial efforts in obtaining a "spectrum" of a heat pulse phonon flux involved the use of paramagnetic impurities in inorganic crystals. Direct, single-phonon, spin-lattice relaxation processes between the impurity spin levels have been well documented. Thus the frequency-selective absorption of heat pulse phonons by these "probes" has proven to be very useful in characterizing the spectrum. Wigmore[59] vacuum evaporated a heater film and a bolometer film on a MgO crystal containing a small concentration of Fe^{+2}. The spin splitting of the Fe^{+2} center was controlled with an external magnetic field. As the magnetic field was increased, at a constant heater power, the magnitude of the bolometer signal

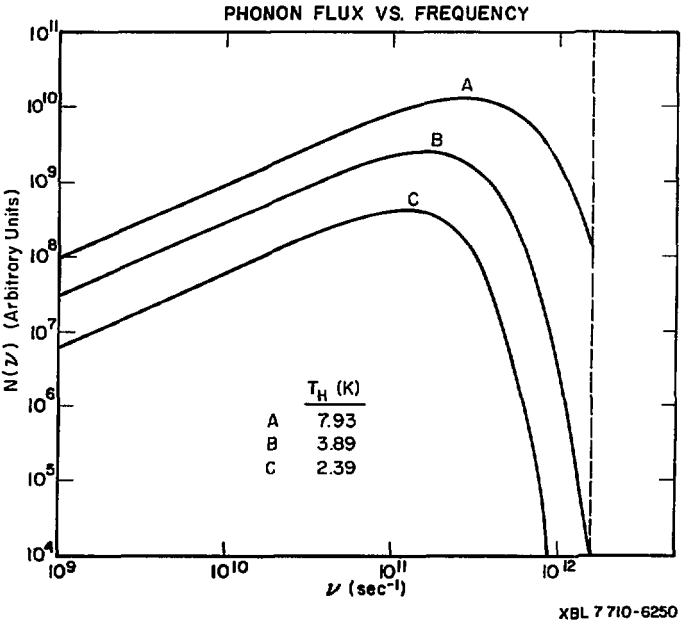

Fig. 15 Spectra of the phonon fluxes from the heater at three different temperatures. The bath temperature is 2.0 K. These particular heater temperatures were calculated from Eq. (32), where $B = 5.0$ mW/cm^2-K^4 and the input powers are, respectively, 1.21 W, 0.064 W, and 0.05 W over an interfacial area of 6 mm^2. The vertical dotted line is the 52 cm^{-1} Debye cutoff of TCB.

decreased until it reached a minimum and then increased again. The minimum in the transmission of the pulse occured at a field strength where the spin splitting was equal to $h\nu_{max}$. Thus a large portion of the heat pulse energy, that which lies in the region of the spectral maximum, was absorbed by the spin system. Since the effective temperature of the heater is $\frac{h\nu_{max}}{2k}$, and since the input power P is known, then Γ can be found from Eq.(29). In this way, Wigmore was able to show that there was a close agreement between the experimental value of Γ and that predicted by the acoustic mismatch of the heater and the MgO crystal. A similar bolometric analysis of the heat pulse spectrum was done by Dynes and Narayanamurti [60], only they used the "stress-tuned" donor levels of Sb in Ge to select phonons from the broad-band flux. It should be noted that in both of these experiments, the crystal sample was directly immersed in the liquid He bath. In each case, the results seemed to indicate that the energy losses to the He bath were negligible in comparison to the flux entering the crystal.

The optical detection of phonon absorption and/or scattering processes in a crystal is a much better method of analyzing the heat pulse spectrum. The sensitivity of a bolometer is restricted to the width of the spectral maximum, which is roughly proportional to kT_H/h. However, if the spin populations can he directly monitored via optical methods, such as circular dichroism, [61] the frequency resolution of the phonon absorption process is restricted only by the width of the spin transition. Anderson and Sabisky[61] were able to show that changes in the circular dichroism associated with the modulation of spin populations in a $SrF_2:Tm^{+2}$ system could be used to analyze the spectrum of the phonons coming from the heater. Their work is particularly relevant to the work undertaken in this thesis because they did not use a heater which was vacuum evaporated onto the crystal. Instead, they used a wire which was wrapped

around one section of the crystal and bonded to it with glyptal cement. The electrical current to the heater was modulated on and off at 20 Hz. The authors demonstrated that the frequencies of the phonons which were absorbed by the spin system under various magnetic field strengths could all be related to the same effective heater temperature. By varying the current to the wire, they also were able to show that the effective heater temperature was proportional to the fourth root of the input power. These results indicated that the resonant phonons were directly radiated by the heater wire, even though the thermal contact between the heater and the crystal was far from ideal.

The technique of phonon spectroscopy is not, of course, limited to paramagnetic spin systems. Renk and Deisenhofer[62] monitored the relative populations of the $\bar{E}(^2E)$ and $2A(^2\bar{E})$ levels of Cr^{+3} ions in AlO_3, which give rise to the well known R_1 and R_2 ruby lines, as a heat pulse propagated propagated through the lattice. Since the energy difference between these excited states is 29 cm^{-1}, they demonstrated that the density of 29 cm^{-1} phonons in the heat pulse could be measured by the relative intensities of the R_1 and R_2 lines. Moreover, since a laser was used to excite the Cr^{+3} ions, they could critically focus on a small section of the crystal; thus the spatial profile of the heat pulse in the crystal was analyzed . A similar technique of phonon spectroscopy was just recently reported by Bron and Grill[63] in their analysis of phonon absorption processes in the vibronic-sidebands of $SrF_2:Eu^{+2}$.

The study of heat pulses has actually gone far beyond the stage of "conventional" black body sources. Many experimentalists have been using superconducting films not only to detect the phonons, but also to generate them.[60,64-66] In these systems, the superconducting quasiparticles are rapidly excited or broken up by electron tunneling in the case of a tunnel-junction generator,

or by a heat pulse in the "phonon fluorescence" technique.[60] The recombination of the particles results in the generation of a phonon energy distribution which is sharply peaked at 2Δ, the energy gap between the normal and superconducting states. Thus a relatively monochromatic flux of phonons will propagate through the crystal. The frequency of the phonons can be tuned by modulating the energy gap with magnetic fields or temperature tuning. The major point to be made in this discussion is that as long as the crystal substrate acts as a good transmission medium, the frequency spectrum of the artificially generated phonons will be a function of the source, whether it is a monochromatic superconducting source or a black body radiator.

Up to now, there have been no attempts to apply the technique of phonon spectroscopy via heat pulses to the study of phonon interactions in molecular crystals. However, Buckley, et. al., have reported [50,67] the observation of optically detected acoustic-paramagnetic-resonance in the chemically-mixed system discussed in Chapter IV, namely h_2-TCB in durene. The important experimental details of the work are as follows.[67] A sweep oscillator supplied microwave power to a thin ZnO transducer vacuum deposited on a short sapphire rod. The acoustic energy propagated down the sapphire rod to the TCB/durene crystal which was bonded to the rod with silicone grease. The acoustic power level in the crystal was estimated to be about 10 mW. Since the excitation/detection arrangement was basically the same as that outlined in the previous chapter, all the experiments were performed by monitoring the TCB phosphorescence origin (3782 Å). In this way they were able to detect triplet spin sublevel transitions when the sweep oscillator scanned through the $D-|E|$, ($\tau_x \leftrightarrow \tau_y$, 3.682 GHz, ,and $2|E|$, ($\tau_y \leftrightarrow \tau_z$, 1.746 GHz), resonances. The absorption spectra indicated that the acoustic energy entered the crystal at the applied fundamental frequency, even though there was

an attenuation of at least 10 dB at the crystal interface. Thus the grease mediated thermal contact did not destroy the monochromaticity of the source. This is an important conclusion in regard to the work presented so far in this thesis, because the acoustic coupling of the heater/crystal interface is essentially the same. Another important observation that was made by Buckley and his co-workers concerned the lifetime of the resonant phonons in the crystal. When the crystal was surrounded by superfluid He, the linewidths of the optically detected acoustic resonances were equal to the inhomogeneous linewidths of the TCB zero-field microwave transitions. Thus there was no indiction that the resonant phonons were being removed from the initial bandwidth of the applied beam before they escaped into the He bath. However, when the He bath was above the lambda point, they observed a definite broadening of the resonances, which indicated that the phonons were scattered out of the applied bandwidth. Hence the poor thermal coupling of the crystal to the normal fluid He prevented the escape of the phonons long enough to make them decay in the crystal.

3. Heat Pulse Absorption by Localized Excited States: Theory

The effective temperature of the nichrome heater used in the molecular crystal experiments is a function of the energy balance between the input electrical power and the phonon radiation co the surrounding media. If there are no thermal losses from the heater film other than through the crystal interface, then the total radiated power in Eq.(29) will be equal to the power dissipated in the film. However, since the heater film is supported by a glass rod, and since the heater/crystal assembly is totally immersed in liquid He, there are additional routes for thermal losses. Thus the value of the heater temperature cannot be calculated directly from the thermal boundary conductivity K_B of the

heater/crystal interface. Instead, one has to formulate a proportionality constant "B," which includes all the radiative losses, such that an effective heater temperature T_{HE} can be calculated from the input power P (= I^2R_H, where R_H is the resistance of the heater film):

$$(32)\quad T_{HE} = \left(\frac{P}{B} + T_B \right)^{\frac{1}{4}} \quad .$$

If a series of different crystals, all having the same geometry, are placed on the heater film, then the only expected change in the proportionality constant B from experiment to experiment should be due to the somewhat variable heater/crystal boundary conductivity. Thus the phonon flux presented in Eq.(30) can be rewritten in terms of the new effective heater temperature T_{HE} and the boundary conductivity K_B :

$$(33)\quad \frac{N(\nu, T_{HE}, T_B)}{A} = K_B \frac{30h^3\nu^2}{\pi^4k^4} \left[\frac{1}{\exp(h\nu/kT_{HE}) - 1} - \frac{1}{\exp(h\nu/kT_B) - 1} \right] .$$

If one assumes that the thermal promotion process involves a single phonon, then a trap state located at an energy (Δ - 4β) below the bottom of the exciton band will be promoted to an intermediate state isoenergetic with the band by the absorption of phonons having energies in the range (Δ - 4β) → Δ. Therefore, the integration of Eq.(33) over the limits of this frequency range will yield the resonant phonon flux for an input power P, given by F(P) in Eq.(34):

$$(34)\quad \frac{F(P)}{A} = \int_{\nu_\ell}^{\nu_h} N(\nu, T_{HE}, T_B)\, d\nu$$

$$= K_B \frac{30h^3}{\pi^4k^4} \left[\xi(T_{HE}) \Big|_{\nu_\ell}^{\nu_h} - \xi(T_B) \Big|_{\nu_\ell}^{\nu_h} \right] \quad \sec^{-1} ,$$

where

$$(35)\quad \xi(T) = \frac{-kT}{h} \exp(-h\nu/kT) \left[\nu^2 + \frac{2kT\nu}{h} + 2\left(\frac{kT}{h}\right)^2 \right]$$

(36) $\nu_{\ell} = (\Delta - 4\beta)/h$

(37) $\nu_{h} = \Delta/h$.

Eq.(34) is obtained from Eq.(33) only after the approximation is made that $h\nu_{\ell}$, $h\nu_{h} > kT_{HE}$, kT_{B}. Thus in order to justify this approximation, the input power to the heater film should be kept as low as possible, such that kT_{HE} is always less than 10 cm^{-1}. This puts a maximum upper limit on T_{HE} of 14 K.

One can now define an absorption coefficient ϕ as the ratio of the relative modulation depth of the trap population to the resonant phonon flux F(P) at a given input power P. If ΔN_{max} is the change in the trap population relative to the steady-state population N_{ss} at temperature T_{B}, then

$$(38)\quad \phi \equiv \frac{(\Delta N_{max}/N_{ss})}{F(P)} \quad .$$

Since the intensity of the phosphorescence emission from the trap is equal to the product of the trap population and the radiative rate constant (see Eq.(6)), then Eq.(38) may be rewritten in terms of the relative phosphorescence modulation depth, evaluated at the end of the heat pulse (Fig.(11)):

$$(39)\quad \phi = \frac{(\Delta I_{max}/I_{ss})}{F(P)} \quad .$$

From Eq.(32) a set of T_{HE} values can be calculated for a given power range and proportionality constant B. This set of effective heater temperatures may then be substituted into Eq.(34) in order to "generate" the power dependence of the phonon flux F(P) which is resonant with the trap-band energy difference. If there is no saturation, spin-lattice relaxation, or trap-to-trap transfer, then

the relative phosphorescence modulation depth will have the same power dependence as the resonant phonon flux F(P).

However, the proportionality constant B, which determines the effective heater temperature for a given input power, is not known a priori. It is difficult, therefore, to predict what the resulting power dependence of $\Delta I_{max}/I_{ss}$ will be for a particular trap. This problem can be solved, however, if the entire procedure just outlined is turned around; that is, from the observed power dependence of $\Delta I_{max}/I_{ss}$ the parameter B can be determined by finding that value of all possible B's which gives the identical phonon flux power dependence. This procedure requires repetitive computer calculations which scan through the flux power dependences for a range of B values and the given values of Δ and 4β, until the correct power dependence is found. Since B contains all the thermal losses from the heater film, the best-fit value should be greater than or equal to K_B (mW/cm^2-K^4). Also, it should be remembered that the effective heater temperatures associated with this value of B and the input power range have to conform to the restriction $kT_{HE} < h\nu_l$, $h\nu_h$. Finally, in order to make a valid comparison of among different traps in different crystals, the set of effective heater temperatures should be reasonably reproducible. In this way, the fluxes of phonons resonant with each trap (e.g. X-trap, hd, h_2 traps), are characterized by the same effective heater temperatures. It will be shown in the next chapter that all of these criteria can be met in the laboratory.

Chapter VI

Heat Pulse Absorption by Localized Excited States: Experimental

1. Introduction

As was outlined at the end of the previous chapter, one can examine the power dependence of the phosphorescence modulation depth $\Delta I_{max}/I_{ss}$ and relate it to the theoretical flux of resonant phonons. The ratio of the modulation depth to the phonon flux, the so-called "absorption coefficient" ϕ , should be constant over a given power range. ϕ is not a true absorption coefficient in relation to that obtained with a spectrophotometer; however, its serves the purpose of normalizing the modulation depth obtained for each trap in a series of different crystals. By normalizing the modulation depths in this way, one is able to reveal the extent to which the density of available band states is important in determining the probablity of trap promotion. One can also make a direct comparison of the X-trap and isotopic trap modulation depths in order to see if the nature of the trap, irrespective of its proximity to the exciton band, plays an important role in the promotion process.

A representative example of the trap phosphorescence modulation depth power dependence for each of the three traps is shown in Fig.(16). The curves are merely the observed power dependences of the "raw" data; the values of $\Delta I_{max}/I_{ss}$ are not normalized with respect to the theoretical phonon fluxes. (The power values on the abscissa scale are over an interfacial area of 6 mm^2). One immediately notices that the X-trap values are significantly lower than either of the two isotopic trap values; thus one can see already that the nature of the trap is going to be important in the analysis of ϕ. The values of $\Delta I_{max}/I_{ss}$ for the

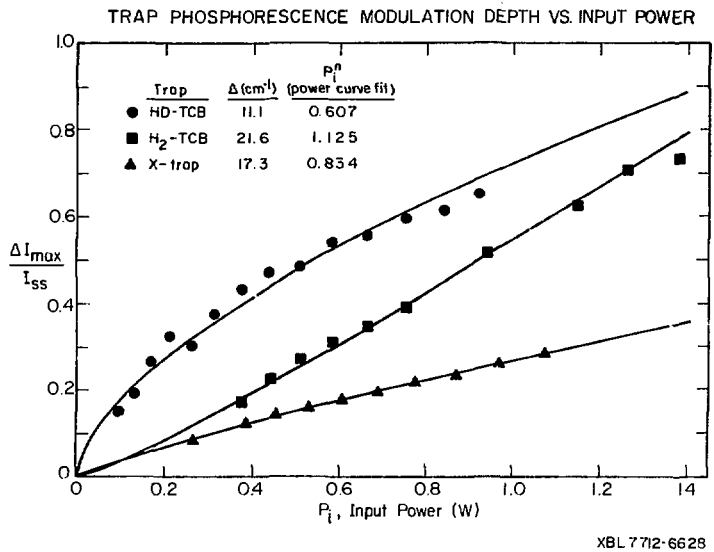

Fig. 16 Power dependence of the relative modulation depth for three traps in TCB. The X-trap is in neat h_2-TCB and the isotropic traps, hd and h_2-TCB, are in d_2-TCB. The input power P_i is over an interfacial area of 6 mm^2.

shallow hd trap are clearly greater than those for the deep h_2 trap in this d_2-TCB crystal. This is what one expects, however, since the flux of phonons resonant with the shallow trap is greater than the higher frequency modes resonant with the deep trap. Finally, the most noteworthy feature is that the depletion of each trap has a unique power dependence which is a function of the trap depth Δ. It will be shown that this arises from the fact that the power dependence of the resonant phonon flux F is a function of Δ and the proportionality constant B.

Since all the raw data to be analyzed in this chapter derive from the same signals which yielded τ_R in Chapter IV, there is a direct correspondence between the respective tables. Thus Table V (ϕ) corresponds with Table II (τ_R) for the X-trap results, and Tables VI and VII correspond to Tables III and IV for the hd and h_2 results.

2. X-trap results

In Table V, each value of B was obtained fitting the observed power dependence of $\Delta I_{max}/Iss$ to an equivalent power dependence of the phonon flux in the energy range $16.0 \rightarrow 17.3\ cm^{-1}$. The effective heater temperatures T_{HE} for each run are shown to the right of the B values. One can see that the maximum value of T_{HE}, corresponding to the maximum power dissipated at the heater film, is always less than the maximum allowable value of 14 K discussed earlier. Since B reflects the "emissivity" of the radiating heater, one can also see that the temperature of the radiator has to be higher, for the same input power , if B is lower.

The average value of B in Table V, excluding that value for sample B where Apiezon N grease was used, is equal to $3.63 \pm 0.89\ mW/cm^2\text{-}K^4$. This is remarkably

Table V: Phosphorescence modulation of X-traps in h_2-TCB
$\Delta = 17.3\ cm^{-1}$, $4\beta = 1.3\ cm^{-1}$

Sample	P range (W/mm^2)	P dependence	B (mW/cm^2-K^4)	T_{HE} range (K)	ϕ $\times 10^{-18}$	ϕ' $\times 10^{-18}$	Band States ±3000
A, 2.0K	0.032-0.315	0.741	2.5	6.02-10.6	0.71±0.25	1.722±0.037	86,000
B, 2.0K	0.047-0.367	0.900	7.2	5.09-8.46	1.32±0.54	1.469±0.058	50,000
C, 2.0K	0.045-0.180	0.834	3.7	5.93-8.38	0.49±0.13	0.923±0.016	47,000
C*, 2.0K	0.055-0.162	0.852	4.0	6.10-7.98	0.54±0.15	0.922±0.019	47,000
C, 1.75K	0.045-0.180	0.868	4.0	5.81-8.20	0.44±0.18	0.772±0.062	47,000
C*,1.75K	0.045-0.180	0.909	5.0	5.50-7.75	0.58±0.21	0.746±0.022	47,000
C, 1.48K	0.055-0.180	0.754	2.5	6.85-9.21	0.22±0.07	0.805±0.018	47,000
C*, 1.48K	0.45-0.180	0.852	3.7	5.92-8.37	0.33±0.12	0.706±0.008	47,000

*h_{2g} emission

close to the coefficient of the grease-mediated heater/crystal interface measured with the bolometer (3.4 mW/cm^2-K^4) and by Connally[34] (3.7 mW/cm^2-K^4). If $B \cong K_B$, then the effective heater temperature T_{HE} is governed primarily by the efficiency of thermal radiation through the heater/crystal interface, and not by direct losses to the other surrounding media such as the heater's glass substrate and the He bath.

If one now considers the values of the absorption coefficient ϕ , there is a disparity between these values and the expected dependence on the number of available band states shown at the far right of Table V. In other words, ϕ is not proportional to the number of band states. This is not surprising in view of the fact that the values of ϕ were calculated from the substitution of the K_B values (mW/cm^2-K^4), presented in Table II, into Eq.(34). These values are not very accurate in the first place, since they were obtained by normalizing the conductances K_B' (mW/K). The normalization of K_B' is valid only if $(T_{HE}-T_B)<T_B$, which is clearly not the case. Thus the values of K_B from Table II should not be used to calculate ϕ. However, if one substitutes the values of B into Eq.(34) instead, the resulting fluxes F'(P) yield absorption coefficients ϕ' which are in much better agreement with the density of band states. Furthermore, if one compares the results for the experiments which monitor the electronic origin with those that monitor the emission to the b_{2g} level, one can see that the ϕ' values are in much better agreement with the notion that the absorption coefficient should be the same for each sublevel in the absence of spin-lattice relaxation processes. The fact that ϕ' gives a much better agreement with theory is consistant with the observation that B is closely related to the thermal conductivity of the heater/crystal interface.

Thus there are two major observations with regard to the X-trap data: (1) The proportionality constant B is very close to the thermal conductivity of the

heater/crystal interface, which indictates that over a 1.0 msec pulse most of the thermal radiation must be propagating through the crystal; and (2) the phonon absorption coefficient ϕ', determined from B instead of K_B, is roughly a function of the density of available band states.

At this time, it is not understood why sample C displays a decrease in ϕ' with decreasing bath temperature. Due to the relatively high effective heater temperatures, the bath temperature makes almost no contribution to the calculated resonant flux. Thus the phonon flux for any given input power is independent of the bath temperature, except at very low input powers (< 0.001 W/mm^2). In Fig.(7), the results are shown for the bath temperature dependence of $\Delta I_{max}/I_{ss}$ observed for sample A at a constant input power of 0.20 W/mm^2. For bath temperatures below 2.0 K, the phosphorescence modulation depth is constant to within 3.3% (0.435 ± 0.014). Hence,there is no bath temperature dependence of the phonon flux in this experiment. (The rapid rise in $\Delta I_{max}/I_{ss}$ near the lambda point of the He bath is coincident with the increase in τ_R of the phosphorescence modulation, also shown in Fig.(8) for the bolometer τ_R, and an increase in the build-up time of the phosphorescence intensity in its return back to the I_{ss} level. Evidently, the heat pulse phonons are not escaping from the crystal into the bath at a rate comparable with the rate they enter at the heater/crystal interface. Thus the crystal is being "filled-up" with phonons due to the loss of thermal coupling between the crystal and the He bath at the lambda point.)

3. Isotopic Trap Results

Table VI contains the results for the analysis of the hd trap in d_2-TCB, where the energy range of the resonant phonon flux is 9.8 → 11.1 cm^{-1}. Unfortunately, results were obtained only for the dilute crystals, where trapping in

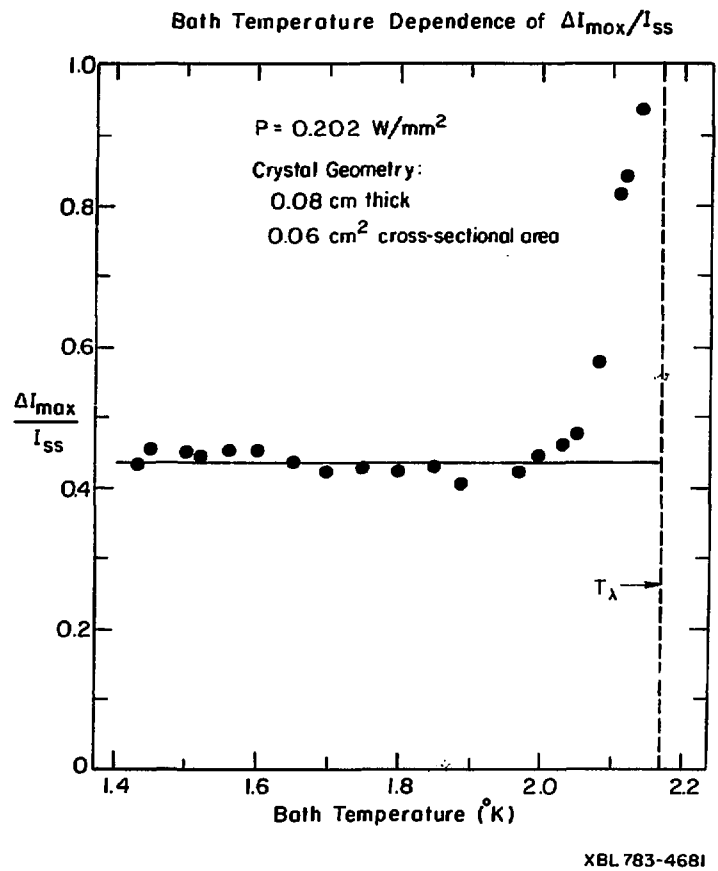

Fig. 17 Bath temperature "dependence" of the relative modulation depth at a constant input power of 0.202 W/mm^2. The straight line drawn through the points taken below 2.0 K is the average value of 0.435 ± 0.014. The rapid rise in the modulation depth near the lambda point is a liquid He effect.

the shallow hd trap is appreciable. The average value of B for these results is somewhat higher (4.45 ± 1.86 mW/cm^2-K^4) than that found for the X-trap, but it is still within the experimental error of the later value. One can also see that lower input powers to the heater film were sufficient to observe the phosphorescence modulation. This expected because the flux of phonons in the resonant energy range at powers of (0.01 → 0.15 W/mm) are comparable to the resonant fluxes in the X-trap range at the higher powers of 0.10 → 0.20 W/mm . (See Table VIII for a complete comparison of the phonon fluxes.)

The h_2 trap results are presented in Table VII, where the resonant phonon flux lies in the energy range of 20.3 → 21.6 cm^{-1}. As in the X-trap case, the absorption coefficients ϕ' for both the hd and h_2 traps were evaluated by substituting the values of B into Eq.(34), in place of the questionable K_B values. When one compares the absorption coefficients of the hd and h_2 traps which are in the same crystal samples, one can see that the hd results are somewhat smaller. A frequency dependence for the absorption coefficient is not expected, since the promotion process is not thought to be a scattering event. The discrepancy may be due to the same thing that plagued the response times τ_R; i.e., there may be energy migration from the h_2 trap to the hd trap during the course of the heat pulse. It is obvious, however, that the absorption coefficients for the two isotopic traps are much greater than those for the X-trap,even though there is always a much higher density of band states in the neat h_2-TCB crystal Thus the data is consistant with the promotion rate constant results mentioned in Chapter II. If the d_2-TCB host/trap ratio truly represents the number of available band states in the isotopic system, then the thermal promotion of the isotopic traps appears to be a factor of 10^3 more efficient than the thermal promotion of X-traps.

Table VI: Phosphorescence modulation of hd-traps in d_2-TCB

$\Delta = 11.1\ cm^{-1}$, $4\beta = 1.3\ cm^{-1}$

Sample	Trap conc.	P range (W/mm^2)	P dependence	B (mW/cm^2-K^4)	T_{HE} range (K)	$\phi' \times 10^{-18}$	Host molecules/trap
D, 2.0 K	1.16% hd, 0.23% h_2	0.016-0.16	0.607	3.5	4.64-8.12	2.115±0.079	72
E, 1.7 K	0.88% hd, 0.04% h_2	0.028-0.06	0.578	2.3	5.91-7.17	2.58 ±0.05	110
E, 1.45 K	"	0.028-0.11	0.679	6.0	4.67-6.55	2.54 ±0.10	110
F, 1.50K	"	0.011-0.14	0.735	6.0	3.68-6.93	2.32 ±0.18	110

Table VII: Phosphorescence modulation of h_2-traps in d_2-TCB

$\Delta = 21.6\ cm^{-1}$, $4\beta = 1.3\ cm^{-1}$

Sample	Trap conc.	P range (W/mm^2)	P dependence	B (mW/cm^2-K^4)	T_{HE} range (K)	$\phi' \times 10^{-18}$	Host molecules/trap
D, 2.0°K	1.16% hd, 0.23% h_2	0.063-0.230	1.125	6.3	5.63-7.77	2.55± 0.076	72
D, 1.70°K	"	0.140-0.230	1.129	9.3	6.23-7.05	2.74±0.13	72
E, 1.80°K	0.88% hd, 0.04% h_2	0.147-0.207	0.964	4.8	7.43-8.09	3.46±0.12	110
E, 1.70°K	"	0.147-0.207	0.95*	4.5±1.9	7.5 - 8.2	3.08±0.34	110
E, 2.0°K	"	0.139-0.207	0.96*	4.5±1.9	7.4 - 8.2	2.56±0.26	110
G, 1.50°K	1.42% hd, 0.78% h_2	0.067-0.193	1.07*	4.5±1.9	6.2 - 8.1	1.17±0.14	42
G, 2.00°K	"	0.102-0.176	1.02*	4.5±1.9	6.9- 7.9	1.89±0.52	42
H, 1.5°K	1.6% hd, 5.4% h_2	0.067-0.114	1.13*	4.5±1.9	6.2- 7.1	0.94±0.18	14
H, 2.0°K	"	0.067-0.143	1.09*	4.5±1.9	6.2- 7.5	0.83±0.16	14

* Average power dependence obtained with extrapolated B = 4.5 ± 1.9 mW/cm^2-K^4
(T_{HE} is also obtained from extrapolated B)

Table VIII: Comparison of the resonant phonon fluxes for the hd, X-trap, and h_2 traps
^4B = 4.5 mw/k^{4}cm^2, T_B = 2.0°K

All values × 10^{20} sec^{-1}

P (W/mm^2)	T_{HE} (°K)	(hd trap)$_{-1}$ 9.8-11.1 cm	(X-trap) $^{-1}$ 16.0-17.3 cm^{-1}	(h_2 trap)$_{-1}$ 20.3-21.6 cm^{-1}
0.017	4.43	0.85	0.29	0.11
0.034	5.24	1.44	0.67	0.33
0.051	5.78	1.89	1.04	0.56
0.068	6.21	2.27	1.38	0.81
0.083	6.56	2.58	1.70	1.05
0.100	6.87	2.86	1.99	1.28
0.117	7.13	3.11	2.27	1.51
0.133	7.37	3.33	2.53	1.74
0.150	7.59	3.53	2.78	1.95
0.170	7.80	3.72	3.02	2.16
0.183	7.98	3.89	3.25	2.37
0.200	8.16	4.05	3.46	2.57
0.217	8.32	4.20	3.68	2.76
0.233	8.47	4.34	3.87	2.95
0.250	8.62	4.48	4.06	3.14

P dependence:	P^t, hd	P^t, X-trap	P^t, h_2
0.017-0.133 W/mm^2	0.654	1.033	1.299
0.133-0.250	0.471	0.747	0.940
0.017-0.250	0.595	0.943	1.186

* Average experimental value for all three traps.

Due to the large amount of scatter in each of the last six h_2 trap power dependences, the results fc these sets of data had to be extrapolated with the average value of B calculated from all the previous experiments (X-trap,hd, and h_2). The error in this average value ($B = 4.5 \pm 1.9$ mW/cm^2-K^4) is transmitted to the error in ϕ'. Despite the lack of precise curve-fitting, there is a definite trend of a decreasing absorption coefficient with the reduction in the number of host d_2-TCB molecules per isotopic trap. Thus it appears that this ratio may in fact represent the true density of band states for the isotopic system. One can also conclude then that the promotion process is dependent on the number of available band states in both the X-trap and isotopic trap systems.

It is possible that the anomalc sly high value of ϕ' in the 5.4% h_2 crystal may he due in part to direct h_2-to-hd excitation transfer. However, this process would require the existence of a set of real or virtual states approximately 11 cm^{-1} above the 22 cm^{-1} h_2 trap and isoenergetic with the hd trap.[13,15] If one examines the calculated fluxes for the resonant phonons in the 11 cm^{-1} range and the 22 cm^{-1} range (Table VIII), one can see that the flux of phonons in the lower energy range does not greatly exceed the flux in the higher range at the powers used to observe the h_2 trap modulation (0.07 → 0.14 W/mm^2). Thus in order to observe appreciable direct trap-to-trap transfer under these conditions, either the density of these real or virtual states must comparable with that in the band, or the phonon-trap coupling leading to these states is more efficient. It is hard to say then if direct trap-to-trap transfer is occuring in this crystal, especially since no states between the h_2 trap and the d_2-TCB have ever been observed.

4. Spectral Resolution

Each trap in the TCB lattice was shown to select a band of phonons within the black body spectrum of the heater radiation which corresponded to the trap depth below the host exciton band. The manifestation of this phenomenon was the particular power dependence associated with the phosphorescence modulation depth for each trap. Although there was a fairly large spread in the fitting parameter B among the various power dependences (4.5 ± 1.9 mW/cm^2-K^4), the spread in the effective heater temperatures is considerably smaller, since $T_{HE} \propto (P/B)^{\frac{1}{4}}$. Thus the results were consistant with the notion that the phonon spectrum is characterized by an effective heater temperature common to all the experiments.

If the depletion of the trap population was in fact not a resonance interaction, but instead was a process that could be effected by any phonon having an energy greater than or equal to the trap depth, then the observed power dependences can be fit only if $B \ll 1.0$ mW/cm^2-K^4. This result is inconsistant with the original condition that $B \geq K_B$. Therefore, one may point to this inconsistancy and conclude that phonons having energies greater than Δ are not involved in the promotion of trapped excitations.

If the $P^{0.943}$ dependence of the X-trap modulation depth in Table VIII was associated instead with the $9.8 \rightarrow 11.1$ cm^{-1} energy range, then the best-fit value of B would be 41.7 mW/cm^2-K^4, instead of 4.5 mW/cm^2-K^4. Similarly, if the same power dependence was associated with the $20.3 \rightarrow 21.6$ cm^{-1} energy range, the best-fit value of B would be 1.7 mW/cm^2-K^4. Thus there is a significant "resolution" among the three trap energy ranges, which would allow one to assign the correct energy range of the trap if the value of B is accurately known from previous experiments. However, the resolution for any particular trap level is no better than the error found in the spectroscopic determination of the trap

depth Δ ($\pm$ 0.4 cm^{-1}). In Table IX one can see that the value of the best-fit B does not change appreciably if Δ varies by only a few tenths of a wavenumber. Thus the precision in the absorption coefficient ϕ' is limited by the precision in Δ. Only can also see from Table X, that the value of B does not change much with the exciton bandwidth 4β; however, the value of ϕ' will reflect the reduction or increase in the resonant flux if 4β is changed. Since the value of 4β has an error[11] of only $\pm$ 0.10 cm^{-1}, the resulting error in ϕ' is not very great.

5. Multiphonon Processes

If the trap phosphorescence modulation was not due to a direct single-phonon absorption process exclusively, but also involved a significant contribution from multiphonon processes, then one would expect the power dependence to reflect this contribution. Two-phonon processes of the Raman type involve the absorption of a phonon having an energy greater than the trap depth and the simultaneous emission of a lower energy phonon, where the energy difference between the two phonons is equal to the trap depth. There are obviously many different combinations of phonons in the heat pulse flux which could fulfill this energy requirement; however, it has already been shown that the power dependence of the flux of phonons with energies greater than the trap depth does not correlate with the observed power dependence of the phosphorescence modulation. Furthermore, the Raman process requires a virtual state above the exciton band which in turn has to couple with the exciton band in order to create the low energy phonon. Since there are no real triplet levels above the band that have been observed in the TCB systems, there is little chance for a resonance enhancement of the Raman process. Thus one could conclude that unless the density of phonons having energies greater than the trap depth greatly exceeds the density of phonons

Table IX: Variation in B with Δ (trap depth)
4β=1.3 cm^{-1} Sample C, X-trap origin, 2.0 K

Δ (cm^{-1})	B (mW/cm^2-K^4)	ϕ' $\times 10^{-18}$ ($\pm$ 0.016)
16.8	4.0	0.866
16.9	4.0	0.873
17.0	3.8	0.887
17.1	3.8	0.894
17.2	3.7	0.908
17.3	3.7	0.923
17.4	3.5	0.930
17.5	3.3	0.946
17.6	3.3	0.953
17.7	3.3	0.960

Table X: Variation in B with 4β (exciton bandwidth)
Δ=17.3 cm^{-1} Sample C, X-trap origin, 2.0 K

4β (cm^{-1})	B (mW/cm^2-K^4)	ϕ' $\times 10^{-18}$
0.50	3.3	2.497 $\pm$ 0.042
1.00	3.5	1.214 $\pm$ 0.021
1.20	3.7	0.995 $\pm$ 0.017
1.30	3.7	0.923 $\pm$ 0.016
1.40	3.7	0.847 $\pm$ 0.014
2.00	4.0	0.570 $\pm$ 0.010
4.00	5.3	0.249 $\pm$ 0.004

actually resonant with the trap-band energy difference, Raman type processes would not be favored. One can see from the spectral density curves in Fig.(15), where B = 5.0 mW/cm^2 - K^4, that the density of phonons greater than than the average trap depth of 15 cm^{-1} (≃400 GHz) dramatically falls off, even at the relatively high heater temperature of 8.0 K.

The same kind of argument could be made concerning the transition probability of a process which involved the simultaneous absorption of two phonons , where the sum of the phonon energies equals the trap depth. Again, there are many combinations of low energy phonons which could effect this process (e.g. $\frac{1}{2}\Delta$ + $\frac{1}{2}\Delta$, 2/3 Δ+ 1/3Δ,...); but each transition would require the presence of a virtual state between the trap state and the band. The virtual states are not close enough to any real (observed) states for resonance enhancement to be helpful. One system where it may be possible to observe two-phonon absorption is the 50 cm^{-1}, chemically-induced Y-trap in TCB. Since the trap depth is practically equal to the Debye cutoff energy of the TCB lattice (θ_D = 52 cm^{-1}), a single-phonon direct process would not be very likely.(The effect of dispersion would also have to be taken into account.) One problem that one may encounter in this experiment is the fact that phonon scattering may obscure the risetime and the power dependence. The scattering would arise not only from the presence of the chemical impurtites (e.g.,para-dichlorobenzene), but also from other phonons, since very high densities would be required to see the transition. Thus it is hard to say at this point whether multiphonon processes can be investigated with the heat pulse technique.

6. Energy Dispersion in the Exciton Band

Since the density of states in the exciton band is not uniform from the

bottom ($K = \pm \pi/a$) to the top ($K = 0$), one might anticipate that not all the phonons in the energy range $(\Delta - 4\beta) \rightarrow \Delta$ would be favored equally to induce thermal promotion. From Eq.(1), the density of states in the exciton band is given by:

$$(40)\quad \rho_E = (1/\sin Ka)$$

Thus the high density of states at the top and bottom of the band, relative to the middle of the band, may cause a greater number of phonons to be absorbed which have energies close to Δ and $(\Delta - 4\beta)$. An attempt was made to see if a reduction in the number of phonons which induce promotion to the middle of the band would effect the power dependence of the resonant phonon flux. Any change in this power dependence would be reflected in the observed power dependence of the phosphorescence modulation depth, which in turn may yield a different value for the proportionality constant B. Therefore a reduction factor was formulated such that the "new" resonant flux, as seen by a trap, of phonons of frequency ν is given by:

$$(41)\quad N'(\nu,T_{HE},T_B) = N(\nu,T_{HE},T_B)\left\{1 - \left[\sin\,(\nu - \nu_\ell)\left(\frac{\pi}{\nu_h - \nu_\ell}\right)\right]\right\}$$

In the above equation, one can see that the flux of phonons whose energies correspond to the top (ν_h) and bottom (ν_ℓ) of the band are not reduced, whereas the flux of phonons corresponding to the precise center of the band are reduced to zero in this approximation. As in Chapter V, ν_ℓ is equal to $(\Delta - 4\beta)/h$ and ν_h is equal to Δ/h. If one lets $p = (\pi/(\nu_h - \nu_\ell))$, then the total "reduced" phonon flux is given by Eq.(42).

$$(42)\int_{\nu_\ell}^{\nu_h} N'(\nu,T_{HE},T_B)d\nu = \int_{\nu_\ell}^{\nu_h} N(\nu,T_{HE},T_B)d\nu - \int_{\nu_\ell}^{\nu_h} N(\nu,T_{HE},T_B)\sin\,(\nu - \nu_\ell)p d\nu$$

The solution to the second integral on the right-hand side of Eq.(42) is very long , thus it will not be presented here. However, the power dependence of the new resonant flux was calculated in the same manner as described earlier. The results seem to indicate that exactly the same B values are needed to fit the phosphorescence modulation depth power dependences (differences show up only in the second decimal place of the mW/cm^2-K"scientific notation). Thus dispersion in the exciton band does not seem to alter the value of the effective heater temperature, or the power dependence of the resonant phonon flux. Since the heat pulse technique relies on the fitting of observed power dependences, no information regarding the band dispersion can be obtained. It may be possible, however, to observe an effect if the bandwidth is much larger than 1.3 cm^{-1}. A possible canditate for an experiment of this sort would be 1,4-dibromonaphthalene, which has a bandwidth of 30 cm^{-1}, [68] and has numerous traps ranging from 28 cm^{-1} to 146 cm^{-1}.

Concluding Remarks

This thesis should be looked upon as the first attempt to understand in detail the phenomenon of heat pulses in molecular crystals. A great deal of time was spent in formulating a reasonable model from the experimental results and the current theories of heat pulse transmission. Much of what was presented could be interpreted differently. However, the author hopes that the reader is convinced that the analysis of heat pulse-induced energy transfer processes in molecular crystals not only provides one with a better understanding of the nature of these phonon-mediated processes, but also gives a better insight into the actual nature of the heat conduction in the crystal.

The experimental results indicate that if relatively pure crystals are used, then the propagation of heat pulse phonons in the crystal can be described in terms of ballistic heat flow. This conclusion cannot be based solely on the analysis of the thermal response time of the heater/crystal system, however. The crucial test is to see if the spectrum of the phonon radiation can be characterized by a reproducible effective heater temperature. Evidence that this is indeed the case was provided by the power dependence of the phosphorescence modulation depth for three distinct traps in the TCB lattice. It is interesting to point out that the same phosphorescence data can then be used to study the the promotion process itself. For the sake of completeness, it would be interesting to measure independently, with a "standard" steady-state technique, the thermal conductivity of the TCB lattice over a much larger temperature range. Another worthwhile experiment along these lines would be to use a different phonon source, such as a superconducting film. If the phonon propagation in the crystal is free of frequency-modulating scattering processes, then it

should be possible to tune the monochromatic phonon generator to the resonant frequency of the trap-band energy exchange.

The main emphasis of the thesis was placed on the desire to show that the heat pulse technique can provide information with regard to the parameters governing the delocalization of trapped excited states. The depletion of the trap population during the course of the heat pulse did in fact show a dependence on the density of available band states and a sensitivity to the nature of the phonon-trap interaction. The problem still remains,however, to explain why the X-trap is much more difficult to delocalize than the isotopic traps. The promotion of the X-trap state probably requires a very different low frequency motion of the associated molecule than that required in the isotopic system. The promotion process may also require a set of local phonon modes which are excited by the heat pulse; in this case, the X-trap may have a very different set of local modes than those found near the isotopic traps. It thus would be an interesting, although perhaps formidable, problem to correlate model calculations of the molecular motions with the results of the relative phonon absorption coefficients.

Finally, the study of heat pulses in molecular crystals should be extended further than trap-phonon interactions. One possible area may be the study of exciton-phonon coupling in a wide-band system such as 1,4-dibromonaphthalene.

Acknowledgements

This work would never have reached its present form without the patience and confidence extended to me by my advisor, Professor Charles B. Harris. I am equally grateful for his financial support for 4½ years.

Professor A. H. Francis was very helpful in providing various thin-film devices, without which the experimental work could have involved a considerable amount of additional effort. I would like to acknowledge the privilege I had of working in Professor Norman Phillips' laboratory; the technical assistance of his student Jim Boyer was also invaluable for the heat capacity work.

I wish to point out that Marc Tarrasch was involved in all of the initial experiments. Although we had very nebulous ideas and questionable data more often than *not, we still had a good time working together.* I am very fortunate to have been able to share my graduate school experiences with him, scientific and otherwise. I am also lucky to have been in the same group with John Brock and Bob Shelby; my admiration for their approach to scientific problems was a basis for my education.

Special thank go to Paul Cornelius for proofreading the manuscript.

This work was supported in part by the Division of Chemical Sciences, Office of Basic Energy Sciences, U. S. Department of Energy, and in part by a grant from the National Science Foundation.

References

1. J. Frenkel, Phys. Rev. 37, 17, 1276 (1931).

2. A. S. Davydov, Theory of Molecular Excitons (New York: McGraw-Hill, 1962).

3. G. F. Koster and J. C. Slater, Phys. Rev. 95, 1167 (1954).

4. G. C. Nieman and G. W. Robinson, J. Chem. Phys. 37, 2150 (1962); 39, 1298 (1963).

5. M. D. Fayer and C. B. Harris, Phys. Rev. B 9, 748 (1974); Chem. Phys. Lett. 25, 149 (1974).

6. S. J. Hunter, H. Parker, and A. H. Francis, J. Chem. Phys. 61, 1390 (1974).

7. A. I. Attia, B. H. Loo, and A. H. Francis, J. Chem. Phys. 61, 4527 (1974).

8. A. H. Francis and C. B. Harris, J. Chem. Phys. 57, 1050 (1972).

9. C. Dean, M. Pollak, B. M. Craven, and G. A. Jeffery, Acta Crysta. 11, 710 (1958); G. Gafner and F. Herbstein, Acta Crysta. 13, 702 (1960).

10. J. Jortner, S. A. Rice, J. L. Katz, and S.-I. Choi, J. Chem. Phys. 42, 309 (1965).

11. A. H. Francis and C. B. Harris, Chem. Phys. Lett. 9, 181, 188 (1971).

12. D. D. Dlott and M. D. Fayer, Chem. Phys. Lett. 41, 305 (1976).

13. M. T. Lewellyn, A. H. Zewail, and C. B. Harris, J. Chem. Phys. 63, 3687 (1975).

14. R. M. Shelby, A. H. Zewail, and C. B. Harris, J. Chem. Phys. 64, 3192 (1976).

15. John C. Brock, Chem. Phys. Lett. XX, XXXX (1978).

16. R. M. Shelby, private communication.

17. R. J. von Gutfeld, in Physical Acoustics, ed. by W. Mason (New York: Academic Press, 1969), vol. V, pp. 233-289.

18. R. J. von Gutfeld and A. H. Nethercot, Phys. Rev. Lett. 12, 641 (1964).

19. R. M. Kimber and S. J. Rodgers, Cryogenics 13, 350 (1973).

20. C. L. Bertin and K. Rose, J. Appl. Phys. 42, 162 (1971).

21. J. K. Wigmore, J. Appl. Phys. 41, 1996 (1970).

22. See, for example: P. C. Kwok, Phys. Rev. 175, 1 :8 (1968); S. J. Rodgers, Phys. Rev. B 3, 1440 (1971); C. C. Ackermann and R. A. Guyer, Ann. Phys. (N.Y.) 50, 128 (1968); H. Beck and R. Beck, Phys. Rev. B 8, 1669 (1973).

23. J. Callaway, Phys. Rev. 113, 1046 (1959); Phys. Rev. 122, 787 (1961).

24. R. Berman, Cryogenics 3, 215 (1963).

25. P. Klemens, in Thermal Conductivity, ed. by R. Tye (London: Academic Press, 1969), vol. 1, pp. 1-68; P. Klemens, Proc. Phys. Soc. A 68, 1113 (1955).

26. R. Berman, Thermal Conduction in Solids (Oxford: Clarendon Press, 1976), pp. 73-103.

27. C. Walter and R. Pohl, Phys. Rev. 131, 1433 (1963).

28. Handbook of Chemistry and Physics (50th ed.; Cleveland: The Chemical Rubber Co., 1969-70), pp. B267-B561.

29. P. L. Kapitza, J. Phys. U. S. S. R. 4, 181 (1941).

30. G. L. Pollack, Rev. Mod. Phys. 41, 48 (1969).

31. W. A. Little, Can. J. Phys. 37, 334 (1959).

32. J. K. Wigmore, Phys. Rev. B 5, 700 (1972).

33. R. E. Jones and W. B. Pennebaker, Cryogenics 3, 215 (1963).

34. J. I. Connally, W. R. Roach, and R. J. Sarwinski, Rev. Sci. Inst. 36, 1370 (1965). The measurements reported here were taken at temperatures below 0.20 K; however, the T^3 dependence of their results indicates that the comparison with the data presented in this thesis is valid. Furthermore, there is no reason why an amorphous material such as vacuum grease should have different properties in the two temperature regions of interest.

35. Charles Kittel, Introduction to Solid State Physics (4th ed.; New York: John Wiley & Sons, Inc., 1971), pp. 215-217.

36. P. A. Reynolds and J. W. White, Disc. Farad. Soc. 48, 131 (1969).

37. L. Van Hove, Phys. Rev. 89, 1189 (1953); Phys. Rev. 93, 1207 (1954).

38. P. A. Reynolds, J. K. Kjems, and J. W. White, J. Chem. Phys. 56, 2928 (1972).

39. G. S. Pawley, Disc. Farad. Soc. 48, 125 (1969).

40. G. S. Pawley and S. J. Cyvin, J. Chem. Phys. 52, 4073 (1970).

41. R. W. Munn and G. S. Pawley, Phys. Stat. Sol. 50, K11 (1972).

42. M. Ito, M. Suzuki, and T. Yokoyama, in Excitons, Magnons, and Phonons, ed. by A. B. Zahlan (Cambridge: University Press, 1968), p. 1.

43. J. R. Scherer, Spectrochim. Acta 19, 1739 (1963).

44. Manufactured by Dow Corning Corporation, Midland, Michigan 48640 U. S. A.

45. For more detail concerning the manufacture of the bolometer films, see H. Parker, K. W. Hipps, and A. H. Francis, Chem. Phys. 23, 117 (1977). The bolometer used in this thesis was kindly supplied by Prof. Francis.

46. American Institute of Physics Handbook of Physics (New York: McGraw-Hill, 1963).

47. William E. Keller, Helium-3 and Helium-4 (New York: Plenum Press, 1969), p. 8.

48. R. D. Williams and I. Rudnick, Phys. Rev. Lett. 25, 276 (1970).

49. Hans Glättli, Can J. Phys. 46, 103 (1968).

50. M. J. Buckley and A. H. Francis, Chem. Phys. Lett. 23, 582 (1973).

51. M. Fooladi, U. S. Patent 3,557,227 (1971).

52. The 98.6% d_2-TCB material was originally prepared by J. C. Brock; the 99.1% d_2-TCB material was supplied by M. D. Fayer.

53. The 0.78% h_2-TCB in d_2-TCB crystal was grown by J. C. Brock; the 5.4% h_2-TCB in d_2-TCB crystal was grown by M. T. Lewellyn.

54. Chorng-Jee Guo and Humphrey J. Maris, Phys. Rev. Lett. 29, 855 (1972); Phys. Rev. A 10, 960 (1974).

55. T. J. B. Swanenburg and J. Wolter, Phys. Rev. Lett. 31, 693 (1973).

56. L. J. Challis, J. Phys. C: Solid State Physics 7, 481 (1974).

57. O. Weis, Z. Angew. Physik 26, 325 (1969).

58. P. Herth and O. Weis, Z. Angew. Physik 29, 101 (1970).

59. J. K. Wigmore, Phys. Rev. B 5, 700 (1972).

60. R. C. Dynes and V. Narayanamurti, Phys. Rev. Lett. 27, 410 (1971); Phys. Rev. B 6, 143 (1972).

61. C. H. Anderson and E. S. Sabisky, in Physical Acoustics, ed. by W. P. Mason (New York: Academic Press, 1971), vol. VIII, pp. 1-57.

62. K. F. Renk and J. Deisenhofer, Phys. Rev. Lett. 26, 764 (1971).

63. W. E. Bron and W. Grill, Phys. Rev. B 16, 5303, 5315 (1977).

64. W. Eisenmenger and A. H. Dayem, Phys. Rev. Lett. 18, 125 (1967).

65. H. Kinder, Phys. Rev. Lett. 28, 1564 (1972); Z. Physik 262, 295 (1973).

66. I. L. Singer and W. E. Bron, Phys. Rev. B 14, 2832 (1976).

67. A. I. Attia, M. J. Buckley, R. M. Panos, and J. M. Raney, Phys. Rev. B 15, 1239 (1977).

68. R. M. Hochstrasser and J. D. Whiteman, J. Chem. Phys. 56, 5945 (1972).